

When, Why and How Much?

Adaptive Learning Rate Scheduling by Refinement

Aaron Defazio
FAIR, Meta

ADEFAZIO@META.COM

Ashok Cutkosky
Boston University

ASHOK@CUTKOSKY.COM

Harsh Mehta
Google Research

HARSHM@GOOGLE.COM

Konstantin Mishchenko
Samsung AI Center

KONSTA.MISH@GMAIL.COM

Abstract

Learning rate schedules used in practice bear little resemblance to those recommended by theory. We close much of this theory/practice gap, and as a consequence are able to derive new *problem-adaptive* learning rate schedules. Our key technical contribution is a refined analysis of learning rate schedules for a wide class of optimization algorithms (including SGD). In contrast to most prior works that study the convergence of the average iterate, we study the last iterate, which is what most people use in practice. When considering only worst-case analysis, our theory predicts that the best choice is the “linear decay” schedule: a popular choice in practice that sets the stepsize proportionally to $1-t/T$, where t is the current iteration and T is the total number of steps. To go beyond this worst-case analysis, we use the observed gradient norms to derive schedules *refined* for any particular task. These refined schedules exhibit learning rate warm-up and rapid learning rate annealing near the end of training. Ours is the first systematic approach to *automatically* yield both of these properties. We perform the most comprehensive evaluation of learning rate schedules to date, evaluating across 10 diverse deep learning problems, a series of LLMs, and a suite of logistic regression problems. We validate that overall, the linear-decay schedule matches or outperforms all commonly used default schedules including cosine annealing, and that our schedule refinement method gives further improvements.

1 Introduction

For minimizing a function f , Stochastic Gradient Descent (SGD) updates the iterate x_t at step t via:

$$x_{t+1} = x_t - \eta_t g_t,$$

where g_t is a (possibly stochastic) sub-gradient at x_t , and η_t is the learning rate (LR) at time t . Choosing a sequence of η_t for steps $t = 1, \dots, T$ is a core problem in optimization.

The learning rate sequence for an optimizer is typically decomposed into two parts: the *baseline* learning rate, indicating the maximum LR to use, and a *schedule*, a sequence that multiplies the baseline LR to give the LR sequence. In this work we focus exclusively on the problem of scheduling. Choosing the right learning rate schedule for best performance is difficult; standard practice is to perform a hyper-parameter sweep over a set of standardized schedules (Wu et al., 2020).

Setting η_t from theory is difficult due to a multitude of potential problem assumptions and the wildly varying schedules that arise from these assumptions. For instance, $\eta_t \propto 1/\sqrt{t}$, $\eta_t \propto 1/t$ and constant schedules $\eta_t = \eta$ are all dictated by three common but different sets of assumptions. Unfortunately, all three work suboptimally in practice for deep learning (Section 3.1), and are unpopular in the community (Ge et al., 2019a). In this work we focus on two causes for this theory-practice gap:

1. Most theory analyzes the average iterate (Polyak, 1990; Ruppert, 1988) $\hat{x}_T = \frac{1}{T} \sum_{t=1}^T x_t$ or a randomly sampled iterate. However, in practice the last iterate x_T is used.

Algorithm 1 Schedule Refinement for SGD

-
- 1: **Input:** $G = \|g_t\|$ sequence of length T , smoothing hyper-parameter $\tau > 0$
 - 2: $\hat{G} = \text{median_filter}(G, \text{filter_width} = \tau T, \text{padding} = (\text{nearest}, \text{reflect}))$
 - 3: Define $w_t = \hat{G}_t^{-2}$
 - 4: **for** $t = 1$ **to** T **do**
 - 5:

$$\eta_t = w_t \sum_{p=t+1}^T w_p$$

- 6: **end for**
 - 7: Return normalized schedule $\eta / \max(\eta)$
-

2. Existing theory for the last iterate often uses crude constant bounds on the gradient norms or curvature. Our new tighter bound involves the entire gradient norm sequence instead, allowing for *problem-adaptive* LR schedules.

Our method is a “refinement” method: it uses a prior training run to produce an improved schedule to use in future runs. The practical variant of our schedule refinement method for SGD is given in Algorithm 1. Given a sequence of gradient norms produced by a prior run, it outputs a new schedule that is adaptive to the structure of the problem. Mathematically, it is minimizing a novel bound we derive on the function value $f(x_T)$ of the final iterate (Section 2.1). The learning rate at each time-step involves a sum of inverse-squared gradient norms from *future* time-steps, a major departure from previous approaches to scheduling.

This approach is partially motivated by the remarkable work of Pan et al. (2022), who show that for the last iterate of quadratic problems, minimizing an upper bound can yield improved schedules. However their work requires knowledge of the full Eigenspectrum of the Hessian, making it impractical to use. Our theory relies on knowledge of the sequence of expected gradient norms, a more tractable quantity.

Our analytical approach also departs from previous approaches by generalizing beyond SGD. Prior analyses of learning rate schedules often rely on the particular form of the SGD iterates to drive the calculations (Jain et al., 2019; Zamani and Glineur, 2023). Our approach is instead a broad technique that provides learning rate schedules for *any* base optimization algorithm. On a technical level, we design a step-size schedule that converts any algorithm which obtains a vanishing regret into one that ensures a last-iterate guarantee. This means that our refinement technique can provide theoretically-motivated schedules for popular base optimization algorithms like Adam.

Overall, we make three main contributions:

1. Theory: We provide an general analysis of learning rate schedules for arbitrary optimization algorithms. Our approach recovers the optimal convergence rates for SGD, and can be used to produce refined schedules customized for a particular task.
2. Practice: Among non-adaptive schedules, we show that warm-up followed by linear decay almost always matches or outperforms other schedules, including cosine decay. Our refined schedules typically provide further improvements, suggesting that our theory provides actionable guidance even for training non-convex neural networks.
3. Theory meets Practice: Our refined schedules exhibit both warmup and nearly-linear decay (Figure 1). While Zamani and Glineur (2023) have very recently shown that linear decay has favorable last-iterate guarantees, to our knowledge this is the first time that warmup has arisen *directly from theory* rather than as an empirical heuristic (Goya et al., 2017). That is, given hindsight knowledge of all gradient statistics, our theoretically optimized schedules usually include a warmup phase during which the learning rate increases.

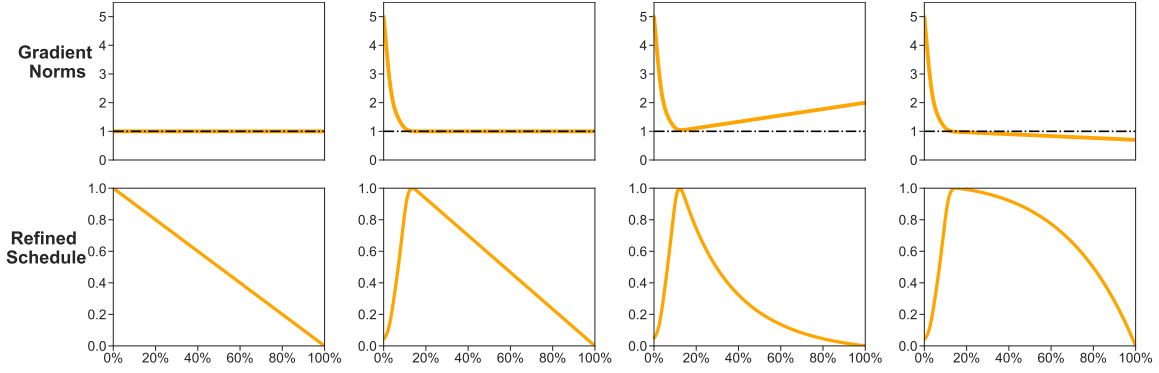


Figure 1: Example gradient norm sequences (top row) and the resulting refined schedules given by Algorithm 1 (bottom row). Black dashed line at $y = 1$ shown for reference. Percentage of runtime on the x-axis.

1.1 Notation

$f: \mathbb{R}^d \rightarrow \mathbb{R}$ is a convex objective. x_1, \dots, x_T and z_1, \dots, z_T are random vectors in \mathbb{R}^d with $x_1 = z_1$, and $\Delta_t \triangleq z_{t+1} - z_t$. Δ_t will indicate “baseline” updates before applying a schedule, and x_t will be iterates after applying the schedule. g_1, \dots, g_T are random vectors in \mathbb{R}^d satisfying $\mathbb{E}[g_t | x_1, \dots, x_t] \in \partial f(x_t)$ ($\mathbb{E}[g_t] = \nabla f(x_t)$ when f is differentiable). G^2 is a bound on $\mathbb{E}[\max_t \|g_t\|^2]$. w_1, \dots, w_T indicate non-negative random variables in \mathbb{R} such that g_t and w_t are independent given x_1, \dots, x_t . We define $w_{a:b} \triangleq \sum_{t=a}^b w_t$. If $a > b$, then $w_{a:b} \triangleq 0$. u denotes an arbitrary element of \mathbb{R}^d ; typically one should consider the case $u \in \arg \min f$. $D \triangleq \|x_1 - u\|$ is the “distance-to-solution” term, and $f_\star \triangleq \inf_u f(u)$.

2 Main Analytical Result

Our general result is Theorem 1. This allows us to convert any sequence z_1, \dots, z_T with bounded regret $\sum_{t=1}^T \langle g_t, z_t - u \rangle$ into a sequence of iterates x_1, \dots, x_T with a bound on $f(x_T) - f(u)$. Thus, Theorem 1 can be viewed as another addition to the family of reductions from stochastic optimization to regret bounds (Cesa-Bianchi et al., 2004; Cutkosky, 2019). The proof can be found in Appendix B.

Theorem 1 *Suppose z_1, \dots, z_T is some arbitrary sequence of vectors. Let w_1, \dots, w_T be an arbitrary sequence of non-negative numbers. Recall that we define $\Delta_t = z_{t+1} - z_t$ and $x_1 = z_1$. For $t \geq 1$, suppose x_{t+1} satisfies:*

$$x_{t+1} = x_t + \frac{w_{t+1:T}}{w_{1:T}} \Delta_t,$$

then for any u :

$$\mathbb{E}[f(x_T) - f(u)] \leq \mathbb{E} \left[\sum_{t=1}^T \frac{1}{w_{1:T}} \langle w_t \cdot g_t, z_t - u \rangle \right].$$

Let us take a moment to consider the implications of this Theorem in the simplest setting of $w_t = 1$ for all t . In this case, it is well-known that by setting $\Delta_t = -\eta g_t$ for $\eta = \frac{D}{G\sqrt{T}}$, one guarantees $\sum_{t=1}^T \langle g_t, z_t - u \rangle \leq DG\sqrt{T}$. Thus, we immediately obtain the following important corollary:

Corollary 2 Set $x_{t+1} = x_t - \eta_t g_t$ with $\eta_t = \frac{D}{G\sqrt{T}} \left(1 - \frac{t}{T}\right)$. Then:

$$\mathbb{E}[f(x_T) - f(u)] \leq \frac{DG}{\sqrt{T}}.$$

Proof With $w_t = 1$ for all t and $\Delta_t = -\frac{D}{G\sqrt{T}}g_t$, classical online gradient descent analysis (Zinkevich (2003)) yields $\sum_{t=1}^T \langle w_t g_t, z_t - u \rangle \leq DG\sqrt{T}$. The result now follows from Theorem 1. \blacksquare

The sequence x_t suggested by Corollary 2 is simply stochastic gradient descent ($x_{t+1} = x_t - \eta_t g_t$) equipped with a *linear decay learning rate schedule*:

$$\eta_t = \frac{D}{G\sqrt{T}} \left(1 - \frac{t}{T}\right). \quad (1)$$

Linear decay emulates the effects of iterate averaging, as the contribution from each gradient to the returned point is approximately the same as it would be in an average: the gradient $g_{T/2}$ appears in half the points in the average, and so its weight is halved, the gradient g_t appears in $T - t$ out of T points and so its weight is $1 - t/T$.

This bound has a significantly better constant than previous schedules for last-iterate convergence of SGD in this setting (Jain et al., 2019), and matches recent work by Zamani and Glineur (2023), who were the first to show that this schedule is actually optimal for gradient descent for the Convex G -Lipschitz complexity class. Our regret analysis recovers their result when specialized to SGD.

In practice, the linear decay schedule is employed not only with SGD but also with a diverse panoply of other optimization algorithms. Our Theorem 1 suggests a theoretical basis for this approach: so long as the underlying optimization method ensures a regret bound, the linear decay schedule will provide a last-iterate guarantee. Note that we do not require the regret bound to be analytically proven (as is the case for e.g. SGD (Zinkevich, 2003), AdaGrad (Duchi et al., 2011; Streeter and McMahan, 2010) or AMSGrad (Reddi et al., 2018)); it suffices for the regret bound to hold in practice (as may hold for Adam (Kingma and Ba, 2015) or AdamW (Loshchilov and Hutter, 2017a)).

The key initial step in the proof of Theorem 1 is an identity we call the “all-tail summation bound”. This is a refinement of a bound from Orabona (2020) who attributes the approach originally to Lin et al. (2016). Using the notation $q_t = f(x_t) - f_*$, Lin et al. (2016) use the bound:

$$w_T q_T \leq \frac{1}{T} \sum_{t=1}^T w_t q_t + \sum_{k=1}^{T-1} \frac{1}{k(k+1)} \sum_{t=k+1}^T w_t (q_t - q_k),$$

whereas our refined approach uses an equality:

$$q_T = \frac{1}{w_{1:T}} \sum_{t=1}^T w_t q_t + \sum_{k=1}^{T-1} \frac{\eta_k}{\sum_{t=k+1}^T \eta_t} \left(\frac{1}{\sum_{t=k}^T w_t} \sum_{t=k}^T w_t (q_t - q_k) \right).$$

This identity is derived in Appendix A. All our results arise from careful manipulation of this identity.

2.1 Optimizing the bound for data-dependent schedules

We have now seen that setting $w_t = 1$ for all t recovers the linear decay schedule, and can obtain the worst-case optimal convergence rates. However, optimizing for the worst case usually yields overly pessimistic behavior. In this section, we build more adaptive schedules that obtain better results on real data. To do this, we simply choose w_t so as to optimize the bound in Theorem 1.

We focus on the particular case of SGD by setting $x_{t+1} = x_t - \eta_t g_t$ with $\eta_t = \frac{w_t w_{t+1:T}}{w_{1:T}}$. In the notation of Theorem 1, this corresponds to $\Delta_t = -w_t g_t$. For this case, we have the following result, with proof in Appendix C.

Theorem 3 Suppose that $x_{t+1} = x_t - \eta_t g_t$ with $\eta_t = \frac{w_t w_{t+1:T}}{w_{1:T}}$. Then we have:

$$\mathbb{E}[f(x_T) - f(u)] \leq \mathbb{E} \left[\frac{1}{2 \cdot w_{1:T}} \left(D^2 + \sum_{t=1}^T w_t^2 \|g_t\|^2 \right) \right]. \quad (2)$$

Moreover, for a fixed sequence $\|g_1\|^2, \dots, \|g_T\|^2$, the value of $\frac{1}{2 \cdot w_{1:T}} (D^2 + \sum_{t=1}^T w_t^2 \|g_t\|^2)$ is minimized by setting:

$$w_t = \|g_t\|^{-2} \frac{D}{\sqrt{\sum_{p=1}^T \|g_p\|^{-2}}}.$$

Theorem 3 suggests that if we knew the sequence of gradient norms ahead of time, then we could optimize the weights w_t (and therefore the learning rate schedule η_t) by setting $w_t \propto \|g_t\|^{-2}$. This yields a simple practical approach for *refining* a learning rate schedule based on empirical observations. First, perform one run using a baseline schedule to observe the sequence of gradient norms. Then, use these norms to compute an optimal schedule via Theorem 3. The constant factor $D = \|x_1 - u\|$ appearing in the value for w_t plays the role of the “scale factor” typically applied to learning rate schedules. A line of recent work has shown that this quantity can be efficiently estimated online without significant downsides (McMahan and Streeter, 2012; Orabona and Pál, 2016; Cutkosky and Orabona, 2018; Mhammedi and Koolen, 2020; Zhang et al., 2022; Carmon and Hinder, 2022; Ivgi et al., 2023; Khaled et al., 2023; Cutkosky et al., 2023).

There are some subtleties here. Allowing w_t to depend on random variable g_t breaks the independence between w_t and g_t . Further, the act of changing the schedule from a baseline to a refined data-dependent schedule will change the gradient norm sequence, which may in turn indicate that a substantially different schedule would have been optimal. Our approach relies on the practical assumption that the gradient norm sequence does not change significantly after refinement. To encourage this, Algorithm 1 applies a median smoothing filter to the gradient norms before refining.

Finally, Theorem 3 provides an analysis that recovers schedules for SGD. However, practitioners commonly use optimization methods with more complicated *per-coordinate* updates or other preconditioning schemes such as Adam. In Appendix E we provide an alternative version of Theorem 3 that applies to such algorithms (Theorem 8). This result enables us to develop schedules tailored to any optimization algorithm. However, actually building this schedule in practice may require inspecting the algorithm’s internal state, which may be difficult or inefficient. For per-coordinate algorithms like Adam, we suggest simply setting $w_t \propto 1/\|g_t\|_1$ as an approximation (see Section 3).

Figure 2.1 gives the Refined schedules on a set of standard benchmark machine learning problems when initially trained using linear decay schedules to provide the gradient norm sequences. Full details of the models and training setup for each problem is provided in the Appendix. Gradient ℓ_2 norms are shown for SGD trained problems (ImageNet, RCNN) and ℓ_1 norms for the Adam trained problems, which also use inverse- ℓ_1 norm weights for refinement (see Section 3). Our single hyper-parameter $\tau = 0.1$ was tuned so that the resulting schedules obtained a balance between smoothness and capturing structure. We recommend setting this parameter *by eye* rather than by grid search.

3 Experiments

To validate the effectiveness of our method on convex problems, we performed a comparison across 8 commonly used classification problems from the LIBSVM repository, with separable problems excluded (see Section 3.5). We used a logistic regression loss together with the Adam optimizer with $\beta = (0.9, 0.95)$, with batch size 16 and trained for 100 epochs. The Refined schedules were calculated by using the linear decay schedule to generate the initial gradient norm sequence. Table 3 demonstrates that both the linear decay schedule and our refinement schedule consistently either match or out-perform the cosine schedule. The linear decay schedule matches the cosine schedule on every problem (up to statistical significance), and

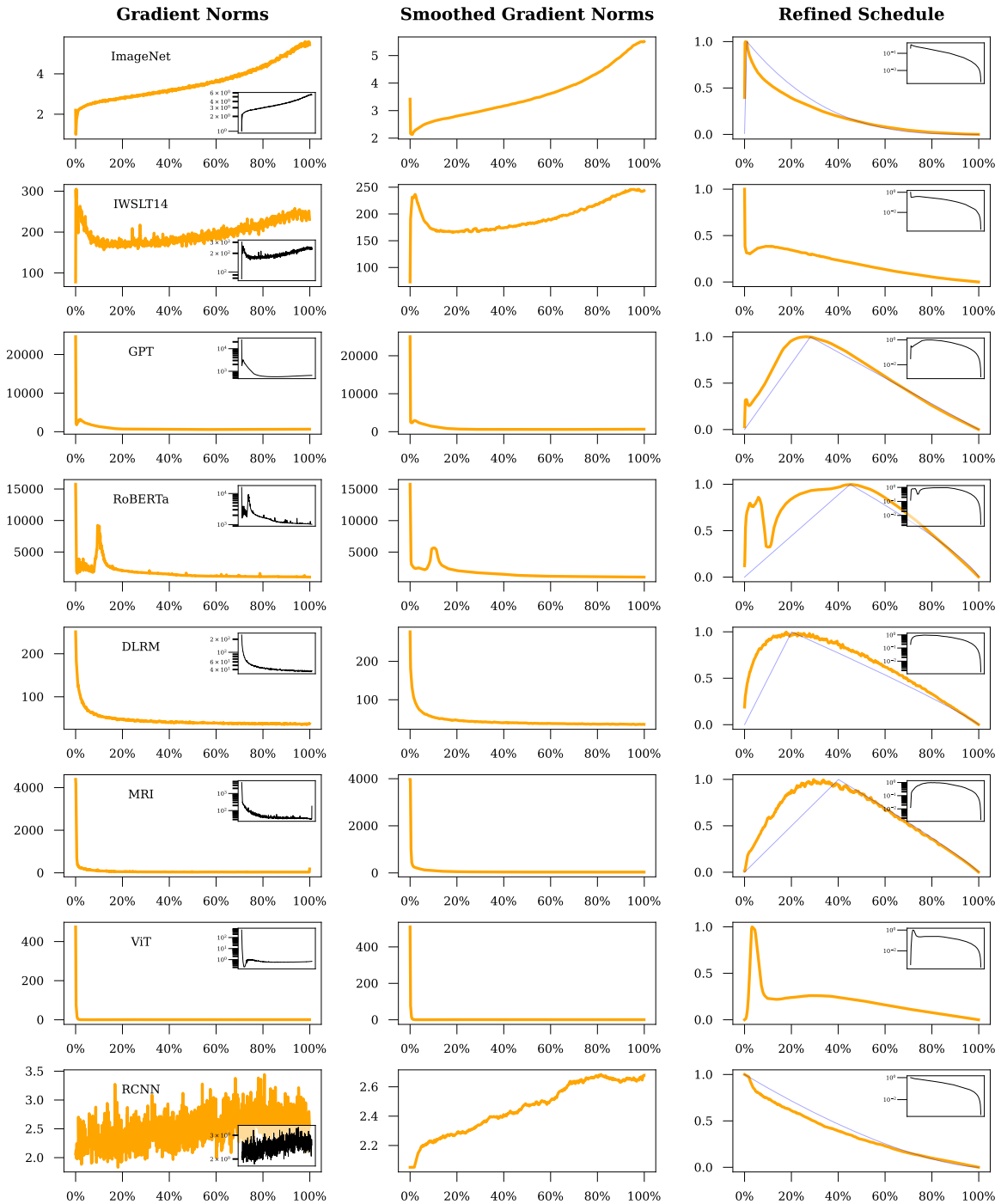


Figure 2: Gradient Norm sequences and the resulting Refined schedules, generated using an initial linear decay schedule with warmup for the initial run. Log scale views are inset for scale reference. Fitted polynomial decay schedules are overlaid in blue.

Table 1: Logistic Regression Experiments (Train Error Rate %).

Problem	Stepwise	Cosine	Linear	Refined $\ g\ _2^2$	Refined $\ g\ _1$	Refined
Aloi	13.38 \pm 0.05	12.69 \pm 0.05	12.76 \pm 0.06	11.75 \pm 0.01	12.24 \pm 0.04	12.30 \pm 0.05
Glass	31.39 \pm 0.16	30.82 \pm 0.22	30.72 \pm 0.18	30.05 \pm 0.44	29.62 \pm 0.37	30 \pm 0.41
Iris	1.39 \pm 0.000	1.39 \pm 0.000	1.39 \pm 0.000	1.46 \pm 0.07	1.46 \pm 0.07	1.46 \pm 0.07
Letter	22.24 \pm 0.008	22.24 \pm 0.01	22.20 \pm 0.02	22.23 \pm 0.03	22.20 \pm 0.03	22.20 \pm 0.03
Pendigits	4.70 \pm 0.02	4.67 \pm 0.01	4.62 \pm 0.03	4.56 \pm 0.02	4.58 \pm 0.02	4.56 \pm 0.04
Sensorless	11.84 \pm 0.09	11.30 \pm 0.09	11.29 \pm 0.09	10.71 \pm 0.08	10.08 \pm 0.05	10.11 \pm 0.05
Vehicle	18.83 \pm 0.09	18.49 \pm 0.05	18.55 \pm 0.06	18.21 \pm 0.12	18.19 \pm 0.08	18.21 \pm 0.1
Vowel	23.43 \pm 0.08	22.99 \pm 0.09	22.94 \pm 0.10	22.48 \pm 0.12	22.44 \pm 0.08	22.41 \pm 0.08

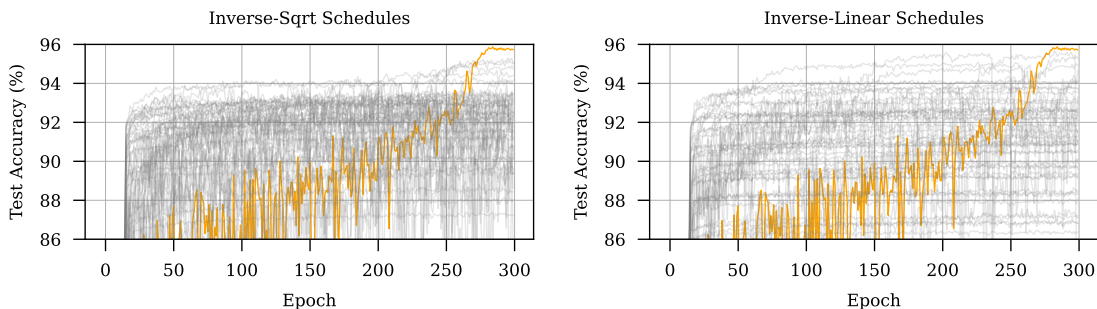


Figure 3: Training curves on CIFAR-10 for a sweep over inverse-sqrt and inverse-linear hyper-parameters. A linear-decay schedule baseline is shown in orange. All combinations are out-performed by the linear-decay schedule.

out-performs it on two problems. The Refined schedule further out-performs the linear decay schedule, either matching or exceeding it across the board.

Rather than using the Adam specific weighting for deriving the Refined schedules, it is often convenient to use other norms, particularly if existing logs are available using these other norms. In Table 3 we present results using both the ℓ_1 norm and ℓ_2 norm-squared weighting. Both are shown to maintain the advantages of the refinement technique, out-performing the non-refined schedules consistently. Given the ease of logging ℓ_1 norms compared to the internal Adam state, we advocate for weights to be the inverse of the ℓ_1 norm (no squaring) when using Adam.

3.1 Deep Learning experiments

Classical any-time learning rates schedules such as $1/\sqrt{t}$ and $1/t$ are commonly used in theoretical analysis of optimization methods, yet they are rarely used by practitioners. To illustrate why, in Figure 3.1, we sweep over the learning rate η and offset β for schedules of the form:

$$\eta \frac{\beta}{\beta + t} \quad \text{and} \quad \eta \frac{\sqrt{\beta}}{\sqrt{\beta} + t}.$$

A 5% duration learning rate warmup was also included in each case. Even with 60 hyper-parameter combinations tried for each family, neither are able to match the performance of the linear-decay schedule. For our deep learning experiments we implemented two commonly used practical variants of these schedules, since sweeping the β hyper-parameter is computationally impractical. The vanilla version uses $\beta = 1$, and the *off-*

set version uses β set to match the duration of the warmup period (a common setting due to its implementation in FairSeq).

3.2 Large-scale schedule benchmark

We performed a large-scale comparison of schedules across common deep learning benchmarks:

CIFAR10 For a small-scale image-classification problem, we chose CIFAR10 (Krizhevsky, 2009). A high-performance Wide ResNet architecture was used (Zagoruyko and Komodakis, 2016). Test error percentage is reported.

CIFAR100 A more realistic yet still small scale benchmark. We used a compact DenseNet architecture (Huang et al., 2017) to increase the diversity of model architectures tested. Test error percentage is reported.

ImageNet We used a ResNet-50 architecture (He et al., 2016) for the ImageNet (Russakovsky et al., 2015) classification task. Note that we used a standard (non-SOTA) data-augmentation pipeline following other recent comparisons in the optimization literature. Test error percentage is reported.

IWSLT14 A small-scale German-English translation task (Cettolo et al., 2014) using a LSTM model (Wiseman and Rush, 2016). Test Perplexity is reported.

GPT A modern small (162M parameter) GPT-style auto-regressive transformer model (Radford et al., 2019) trained on the large Book-Wiki corpus (Zhu et al., 2015). Test Perplexity is reported.

RoBERTa A masked autoencoder variant (Liu et al., 2019) also trained on the Book-Wiki corpus. Test Perplexity is reported.

ViT A high-performance ImageNet classifier using a Vision Transformer (Dosovitskiy et al., 2021). In contrast to our ResNet-50 experiments, here we use modern data-augmentation, following standard practice for ViT training. Test error percentage is reported.

DLRM A modern recommendation system engine (Naumov et al., 2019) trained on the open Criteo Kaggle Display Advertising dataset. Test Accuracy is reported.

MRI A large stacked U-Net architecture (Sriram et al., 2020) trained on the fastMRI dataset (Zbontar et al., 2018), an image-to-image regression task from the medical imaging domain. Test set metric $100 \cdot (1 - \text{SSIM})$ is reported.

RCNN The object detection method Faster-RCNN (Ren et al., 2015) trained on the COCO 2017 dataset, using a ResNet-50 ImageNet pretrained backbone. $100 - \text{box AP}$ is reported.

For each problem, we first performed a sweep of learning rates on a grid $[10^i, 2 \times 10^i, 5 \times 10^i]$ for varying i , separately for each schedule. We then ran multiple seeds using the best learning-rate from the grid search. Mean and standard error of the mean was tabulated for each schedule. The best result for each method, up to a statistical significance level of 0.05 using a paired two-sample t-test, is highlighted in bold. Specific details of the hyper-parameters used for each problem are given in Appendix G. All non-adaptive schedules included a fixed learning-rate warmup, with length following standard practices for the problem. Our stepwise schedule uses a 30-60-90 percent tenting, following standard practices from ImageNet training. As in the convex experiments, the Refined schedules were calculated by using the linear schedule to generate the initial gradient norm sequence.

Tables 2 & 3 show the results. We break the schedules into two categories, classical and modern. The modern schedules consistently outperform the classical schedules, often by large margins. Although this is common folk-law in deep learning, we are not aware of any existing large-scale experiments establishing this. Our comparison of modern schedules shows a clear hierarchy among the schedules. The Stepwise schedule is dominated by the Cosine schedule, and the Linear schedule matches or outperforms the Cosine schedule on all problems except ViT. The refined schedule further outperforms the Linear schedule on 5 of the 10 problems, but shows mixed results on ViT and RCNN. The refinement process produced degenerate schedules that fail on the CIFAR problems, we discuss this in Appendix 3.5.

Table 2: Classical Schedule Comparison Against the Linear Schedule (lower = better).

Problem	Flat	1/t	1/sqrt	Offset 1/t	Offset 1/sqrt	Linear
CIFAR10	8.04 \pm .13	5.42 \pm .28	6.37 \pm .41	9.23 \pm .08	6.58 \pm .06	4.35 \pm .05
CIFAR100	30.43 \pm .20	26.58 \pm .11	29.09 \pm .16	32.80 \pm .07	27.62 \pm .13	22.11 \pm .08
ImageNet	33.00 \pm .14	26.48 \pm .06	28.35 \pm .05	47.94 \pm .08	27.34 \pm .06	23.11 \pm .07
IWSLT14	8.07 \pm .02	7.62 \pm .01	7.52 \pm .01	12.89 \pm .06	8.48 \pm .01	7.10 \pm .01
GPT	20.20 \pm .000	18.99 \pm .04	19.48 \pm .02	27.85 \pm .05	22.88 \pm .006	18.60 \pm .02
RoBERTa	4.52 \pm .005	4.25 \pm .007	4.33 \pm .01	5.33 \pm .02	5.15 \pm .02	3.94 \pm .007
DLRM	20.95 \pm .006	47.59 \pm 6.45	45.99 \pm 5.98	20.94 \pm .007	20.99 \pm .009	20.94 \pm .006
MRI	9.00 \pm .04	8.91 \pm .01	8.98 \pm .04	9.53 \pm .08	9.16 \pm .05	8.88 \pm .02
ViT	30.11 \pm .27	28.36 \pm .40	28.53 \pm .15	73.84 \pm 6.08	50.36 \pm 12.39	24.82 \pm .31
RCNN	65.43 \pm .12	63.38 \pm .05	64.13 \pm .10	79.32 \pm .07	69.25 \pm .07	60.98 \pm .02

Table 3: Modern Schedule Comparison (lower = better).

Problem	Stepwise	Cosine	Linear	Refinement
CIFAR10	4.53 \pm .03	4.27 \pm .04	4.35 \pm .05	-
CIFAR100	22.78 \pm .10	22.59 \pm .09	22.11 \pm .08	-
ImageNet	23.51 \pm .07	23.10 \pm .06	23.11 \pm .07	23.12 \pm 0.03
IWSLT14	7.43 \pm .01	7.17 \pm .009	7.10 \pm .01	6.92 \pm .03
GPT	19.70 \pm .03	18.65 \pm .02	18.60 \pm .02	18.29 \pm .005
RoBERTa	4.36 \pm .01	4.07 \pm .000	3.94 \pm .007	3.86 \pm .005
DLRM	20.95 \pm .008	20.94 \pm .005	20.94 \pm .006	20.94 \pm .009
MRI	8.97 \pm .02	8.90 \pm .03	8.88 \pm .02	8.85 \pm .01
ViT	26.27 \pm .33	24.56 \pm .15	24.82 \pm .31	25.53 \pm .16
RCNN	61.76 \pm .06	61.00 \pm .04	60.98 \pm .02	61.88 \pm .02

3.3 Cosine schedule ablations

To further investigate the failure modes of the cosine schedule, we ran a series of shorter duration training runs on CIFAR10. Our premise was that the cosine schedule is heavily over-fit to long training duration computer vision problems. As shown in Table 4, the cosine schedule begins to under-perform the linear decay schedule and the refined schedules when training for less than 30 epochs. In contrast, while the refined schedule also under-performs for longer duration training it has no statistically significant differences from the linear decay schedule for shorter duration training, where they both perform consistently better than the cosine schedule.

3.4 Large Language Model size ablations

In addition to the results above, we validate our insights on Language Models by performing an additional set of experiments directly comparing to the setting explored in Chinchilla (Hoffmann et al., 2022) where we train a vanilla Transformer model on the C4 dataset (Raffel et al., 2020) for 10k steps with a token batch size of around 524k (2^{19}). Starting with Hoffmann et al. (2022), most recent LLMs employ the AdamW optimizer with Linear Warmup and Cosine Decay. We perform a head-to-head comparison of Cosine decay, Linear decay and Refined schedules (the latter is refined from Linear decay). As shown in Table 5, contrary to popular wisdom, Linear decay performs better than Cosine decay across all model sizes. The Refined schedule outperforms Linear Decay for all but the 3.5B sized model.

Table 4: CIFAR10 Training Time Ablations (Test Error %).

Schedule	1 Epoch	5 Epochs	15 Epochs	30 Epochs
Cosine	35.80 \pm 0.27	15.07 \pm 0.11	7.99 \pm 0.06	6.08 \pm 0.03
Linear Decay	33.84 \pm 0.17	14.36 \pm 0.07	7.65 \pm 0.07	6.12 \pm 0.08
Refined	34.04 \pm 0.19	14.59 \pm 0.08	7.88 \pm 0.04	6.24 \pm 0.06

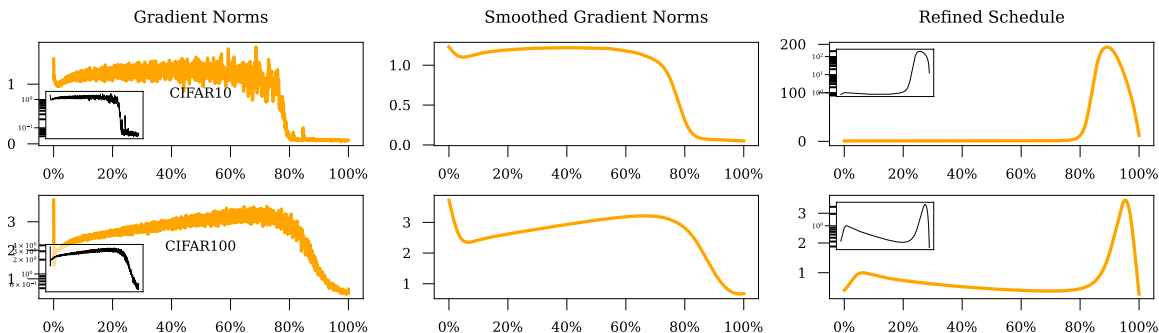


Figure 4: Limitations of refinement: if model over-fits, our method produces degenerate schedules.

3.5 Limitations

The cifar10 and cifar100 problems show potential pitfalls from using our approach (Figure 3.3) when our assumptions break down. On these problems 100% train accuracy is reached near the end, driving the gradient norm sequence to zero. The resulting refined schedule rapidly increases the step size near the end of optimization, which if used results in training divergence. We suggest using a linear decay schedule instead on problems where the gradient norm drops significantly at the end.

4 Discussion

Gradient sequences that slowly decrease or slowly increase after stabilizing are often observed in practice (Figure 2.1), and the resulting schedules that our framework produces show interesting behavior, resembling *polynomial-decay* schedules with exponents p :

$$\eta_t \propto \left(1 - \frac{t}{T}\right)^p. \quad (3)$$

Schedules of this form are already in use, with p typically tuned as a hyper-parameter. From Figure 1, we see that $p < 1$ should be used when the gradient norm is decreasing over time, $p > 1$ when the gradient norm is increasing, and $p = 1$ when the gradient sequence is flat. We use the term *polynomial decay* for the schedule given in Equation 3, which its name in both PyTorch and Tensorflow, although in the literature schedules of the form $1/t^\alpha$ are also sometimes referred to as polynomial schedules. From Figure 2.1, we can see that many of our test problems have refined schedules that are well-approximated by a polynomial decay sequences, shown in blue.

5 Related work

The Robbins-Monro conditions are the foundation of early learning rate theory (Robbins and Monro, 1951). They advocated for step size sequences where $\sum_{t=1}^{\infty} \eta_t = \infty$ and $\sum_{t=1}^{\infty} \eta_t^2 < \infty$. Of the schedules satisfying these conditions, they advocated for schedules with $1/t$ decay as they are asymptotically optimal for twice

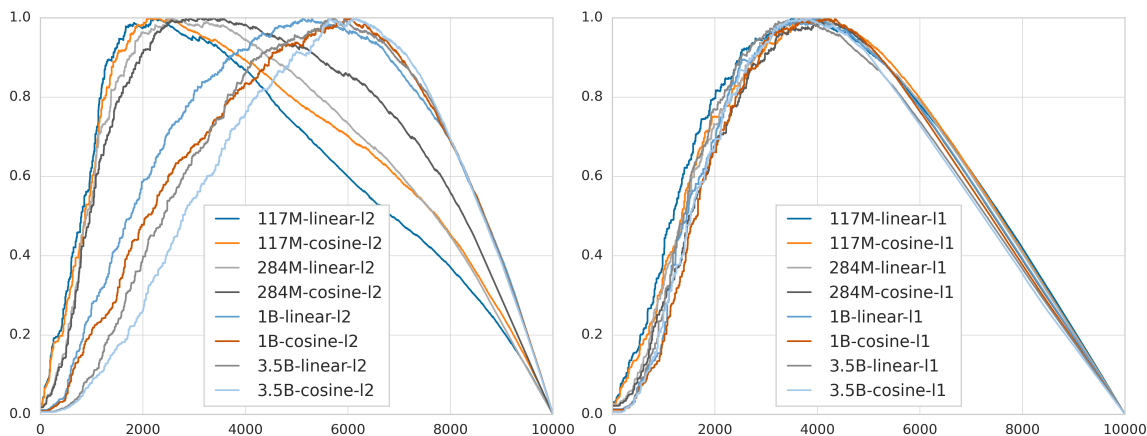


Figure 5: Normalized learning rate schedules learned on vanilla Transformer-based LLM trained on C4 dataset. Left: schedules obtained when setting $w_t \propto \|g_t\|^{-2}$. Right: schedules when $w_t \propto 1/\|g_t\|_1$. We find that ℓ_1 norm is much more consistent across model sizes and baseline schedules. Thus, we used $w_t \propto 1/\|g_t\|_1$ weighting from linear baselines to obtain Refined schedule mentioned in Table 5. The x axis is training steps.

Table 5: LLM Ablations (C4 validation loss).

Schedule	117M	284M	1B	3.5B
Cosine	3.089	2.891	2.729	2.631
Linear Decay	3.087	2.888	2.725	2.625
Refined	3.075	2.884	2.722	2.634

continuously differentiable and strongly convex functions. This schedule was later shown to be optimal (even non-asymptotically) for strongly convex G-Lipschitz stochastic optimization when appropriate averaging is used (Shamir and Zhang, 2013; Lacoste-Julien et al., 2012; Rakhlin et al., 2012).

Nemirovski et al. (2009) point out that the performance of these step-sizes is extremely poor when the base step size is miss-specified, and advocate $1/\sqrt{t}$ step sizes, which have the advantage of performing asymptotically optimally when strong convexity is not present. The use of $1/\sqrt{t}$ step sizes in combination with averaging was originally developed by Polyak (1990) and Ruppert (1988), and are optimal for the complexity class of G-Lipschitz convex functions with or without stochasticity (Blair, 1985; Nesterov, 2018).

Scheduling for the stochastic quadratic setting has seen significant recent interest. The seminal work of Bach and Moulines (2013) establish that a flat $1/4R$ schedule (for a given problem dependent-constant R), independent of the stopping time T , gives the optimal $\mathcal{O}(1/T)$ rate for the average iterate. For the last iterate, Ge et al. (2019a) establish that the step-decay schedule’s rate:

$$\Theta\left(\frac{d\sigma^2}{T} \log T\right),$$

is a multiplicative log factor worse than the mini-max optimal rate. Here d is the dimensionality of the problem and σ a bound on the noise. They further show that the any-time last-iterate behavior of SGD is poor, visiting highly sub-optimal function values infinitely often. Pan et al. (2022) study the situation where

Table 6: Polynomial Decay Schedules fit to refined schedules

Problem	Warmup	Power
DLRM	20%	0.9
GPT	28%	1.0
RoBERTa	45%	0.8
MRI	40%	0.9
RCNN	0%	1.5
ImageNet	1%	3.0

the full Hessian spectrum is known in advance. In this case, they are able to improve the rate to

$$\mathcal{O}\left(\frac{d\sigma^2}{T} \log \kappa\right),$$

or, under a skewed spectrum assumption, to

$$\mathcal{O}\left(\frac{d\sigma^2}{T}\right).$$

Ge et al. (2019b) show that commonly used schedules such as polynomial decay schedules are sub-optimal in the quadratic setting.

5.1 Non-smooth last iterate convergence

For non-smooth stochastic optimization, Shamir and Zhang (2013) show that the last iterate of SGD on non-smooth, convex problems with a $1/\sqrt{t}$ step size is

$$\mathcal{O}\left(\frac{\log(n)}{\sqrt{n}}\right).$$

Harvey et al. (2019) show a corresponding lower bound, showing that the log factor is unavoidable when using $1/\sqrt{t}$ step-sizes.

Jain et al. (2019) were the first to show that the log-factor can be removed if the horizon is known in advance. Their approach uses a sequence of step sizes:

$$\gamma_t = \frac{D2^{-i}}{G\sqrt{T+1}},$$

where i is an epoch counter, for a sequence of epochs each half the length of the preceding epoch. This step size sequence gives a convergence rate for the last iterate of:

$$E[f(x_T) - f_*] \leq \frac{15GD}{\sqrt{T}}.$$

For more general conversions from regret bounds to last iterate guarantees, Cutkosky (2019) provides an alternative conversion based upon evaluating gradients at running averages of iterates and achieves the same last-iterate convergence rate as Theorem 1. However, our method is directly interpretable in terms of learning rate schedules to yield immediate practical guidance while the technique of Cutkosky (2019) is a more opaque transformation of the base algorithm. Nevertheless, there are interesting contrasts: the result of Cutkosky (2019) is "anytime" in the sense that each individual iterate comes with an optimal convergence guarantee. In our case, only the last iterate has an optimal guarantee (in fact, Zamani and Glineur (2023) show that this restriction is necessary for any scheme based on learning rate schedules). Understanding the differences in these approaches is a valuable future direction.

PyTorch Scheduler	Github Files (in thousands)
ReduceLROnPlateau	105
StepLR	101
MultiStepLR	37.9
CosineAnnealingLR	37.1
ExponentialLR	16
OneCycleLR	14.9
CosineAnnealingWarmRestarts	10.9
CyclicLR	9.1
LinearLR	5.9
ConstantLR	3.6
MultiplicativeLR	2.6
PolynomialLR	1.3

Table 7: Popularity of standard learning rate schedules

5.2 Schedules in Applications

Learning rate schedules used in applications usually fall within a few standard classes supported by major frameworks. To survey the use of schedulers in open source software, we performed a GitHub search on each of the schedulers in the PyTorch Library. Table 7 shows that the polynomial decay schedule that we advocate is currently the least popular scheduler in PyTorch.

The reduce-on-plateau, and its fixed length sister, the step-wise schedule, popularized by Krizhevsky et al. (2012) for use in image classification, is considered a benchmark method. They justify it heuristically (“The heuristic which we followed was to divide the learning rate by 10 when the validation error rate stopped improving with the current learning rate.”). Due to its use in highly influential papers as well as its use in tutorials, it is by far the most commonly used schedule (Table 7).

Many early works use step-sizes satisfying the Robbins-Monro conditions, such as step sizes proportional to $1/(c + \alpha t)$, for some c and α , as advocated in the influential work of Bottou (1991, 2012). These step sizes produce large values for small t and so are often clipped (using $\min(\beta, \cdot)$ for some β).

Schedules involving restarting (also called cycling) are also widely used, particularly on computer vision problems where overfitting can be an issue (Smith and Topin, 2018). Loshchilov and Hutter (2017b) use restarting together with the cosine annealing schedule:

$$\eta_t = \eta_{\min} + (\eta_{\max} - \eta_{\min}) \left(1 + \cos \left(\frac{t}{T} \pi \right) \right), \quad (4)$$

This schedule is remarkably effective in practice for image classification problems even without restarts; as far as the authors are aware, for ResNet-50 ImageNet training, no schedule has been demonstrated that outperforms it. It is less commonly used in other problem domains. The motivation for the use of cosine function is unstated, and there is no theory to support it. The reasons for the success of the schedule are not currently understood.

The only large-scale comparison of schedulers for deep learning optimization that we are aware of is the work of Schmidt et al. (2021). They compare on a smaller set of problems than our comparison, although across a range of optimizers, whereas we focus on just Adam & SGD.

5.3 Any-time Adaptive Schedules

There has been significant work on any-time learning rate adaptation that makes use of gradient or loss information to adapt the learning rate. Schedules in the AdaGradNorm class are backed by strong theory (Wu et al., 2020; Streeter and McMahan, 2010; Duchi et al., 2011; Ward et al., 2019; Li and Orabona, 2019). They

use step sizes of the form:

$$\eta_t \propto \frac{1}{\sqrt{\sum_{t=1}^T \|g_t\|^2}}$$

They have not seen significant adoption in practice, likely due to the intrinsic disadvantages of any-time $O(1/\sqrt{t})$ -style schedules as already discussed. It is also not clear how to apply this schedule on top of existing high-performance optimizers such as Adam.

Methods based on hyper-gradients (i.e. gradients of the learning rate) are another heavily studied class of any-time adaptive methods. They use recent gradient evaluations and other local information to update the learning rate at each step of training (Almeida et al., 1999; Franceschi et al., 2017; Bengio, 2000; Domke, 2012; Pedregosa, 2016; Baydin et al., 2018; Feurer and Hutter, 2019; Donini et al., 2020; Chandra et al., 2022). The hyper-gradient can also be used in a more cautious manor to define conditions under which the learning rate should be decreased (Pflug, 1983, 1988; Lang et al., 2019; Zhang et al., 2020).

Methods based on loss minimization aim to choose a learning rate that greedily minimize the loss, either at each step, or based on aggregate statistics that are either produced in stages or by smoothing. They include methods that target the train loss or loss on held out validation data (Xu et al., 2019; Jin et al., 2021; Kim et al., 2021).

Methods that query additional points, such as line search methods, are not scheduling methods *per se* but can be used in place of scheduling (Mahsereci and Hennig, 2017; Iyer et al., 2021). Due to the additional implementation complexity and the cost of their use, they also have not seen widespread adoption for deep learning.

Conclusion

Our experimental results strongly support the use of the linear decay schedule as a default baseline for deep learning optimization. Applying refinement on top of an initial linear decay run gives a schedule showing improvements on 5 out of 10 deep learning problems and 5 of 8 convex problems. We develop extensive theory supporting the linear decay schedule and our novel refinement technique, establishing that their SOTA performance is well-supported both in theory and practice.

References

- Luís B. Almeida, Thibault Langlois, José D. Amaral, and Alexander Plakhov. *Parameter Adaptation in Stochastic Optimization*, page 111–134. Cambridge University Press, USA, 1999. ISBN 0521652634. (Cited on page 14)
- Francis Bach and Eric Moulines. Non-strongly-convex smooth stochastic approximation with convergence rate $o(1/n)$. *Neural Information Processing Systems (NeurIPS)*, 2013. (Cited on page 11)
- Atilim Güneş Baydin, Robert Cornish, David Martínez Rubio, Mark Schmidt, and Frank Wood. Online learning rate adaptation with hypergradient descent. In *Sixth International Conference on Learning Representations (ICLR), Vancouver, Canada, April 30 – May 3, 2018*, 2018. (Cited on page 14)
- Yoshua Bengio. Gradient-based optimization of hyperparameters. In *Neural Computation*, 2000. (Cited on page 14)
- Charles Blair. Problem complexity and method efficiency in optimization (a. s. nemirovsky and d. b. yudin). *SIAM Review*, 27(2):264–265, 1985. (Cited on page 11)
- Leon Bottou. Stochastic gradient learning in neural networks. *Proceedings of Neuro-Nimes*, 91(8):12, 1991. (Cited on page 13)
- Léon Bottou. *Stochastic Gradient Descent Tricks*, pages 421–436. Springer Berlin Heidelberg, 2012. (Cited on page 13)

- Yair Carmon and Oliver Hinder. Making sgd parameter-free. In *Conference on Learning Theory*, pages 2360–2389. PMLR, 2022. (Cited on page 5)
- Nicolo Cesa-Bianchi, Alex Conconi, and Claudio Gentile. On the generalization ability of on-line learning algorithms. *IEEE Transactions on Information Theory*, 50(9):2050–2057, 2004. (Cited on page 3)
- Mauro Cettolo, Jan Niehues, Sebastian Stüker, Luisa Bentivogli, and Marcello Federico. Report on the 11th IWSLT evaluation campaign. In *IWSLT*, 2014. (Cited on page 8)
- Kartik Chandra, Audrey Xie, Jonathan Ragan-Kelley, and Erik Meijer. Gradient descent: The ultimate optimizer. In *36th Conference on Neural Information Processing Systems (NeurIPS)*, 2022. (Cited on page 14)
- Ashok Cutkosky. Anytime online-to-batch, optimism and acceleration. In *International conference on machine learning*, pages 1446–1454. PMLR, 2019. (Cited on pages 3 and 12)
- Ashok Cutkosky and Francesco Orabona. Black-box reductions for parameter-free online learning in banach spaces. In *Conference On Learning Theory*, pages 1493–1529. PMLR, 2018. (Cited on page 5)
- Ashok Cutkosky, Aaron Defazio, and Harsh Mehta. Mechanic: A learning rate tuner. *arXiv preprint arXiv:2306.00144*, 2023. (Cited on page 5)
- Justin Domke. Generic methods for optimization-based modeling. In *Fifteenth International Conference on Artificial Intelligence and Statistics (AISTATS)*, 2012. (Cited on page 14)
- Michele Donini, Luca Franceschi, Orchid Majumder, Massimiliano Pontil, and Paolo Frasconi. Marthe: Scheduling the learning rate via online hypergradients. In Christian Bessiere, editor, *Proceedings of the Twenty-Ninth International Joint Conference on Artificial Intelligence, IJCAI-20*, pages 2119–2125. International Joint Conferences on Artificial Intelligence Organization, 7 2020. (Cited on page 14)
- Alexey Dosovitskiy, Lucas Beyer, Alexander Kolesnikov, Dirk Weissenborn, Xiaohua Zhai, Thomas Unterthiner, Mostafa Dehghani, Matthias Minderer, Georg Heigold, Sylvain Gelly, Jakob Uszkoreit, and Neil Houlsby. An image is worth 16x16 words: Transformers for image recognition at scale. In *International Conference on Learning Representations*, 2021. (Cited on page 8)
- John Duchi, Elad Hazan, and Yoram Singer. Adaptive subgradient methods for online learning and stochastic optimization. *Journal of Machine Learning Research*, 12(61), 2011. (Cited on pages 4 and 13)
- Matthias Feurer and Frank Hutter. *Automated Machine Learning*, chapter Hyperparameter Optimization. Springer International Publishing, 2019. (Cited on page 14)
- Luca Franceschi, Michele Donini, Paolo Frasconi, and Massimiliano Pontil. Forward and reverse gradient-based hyperparameter optimization. In *Proceedings of the 34th International Conference on Machine Learning*, volume 70 of *Proceedings of Machine Learning Research*, pages 1165–1173. PMLR, 2017. (Cited on page 14)
- Rong Ge, Sham M. Kakade, Rahul Kidambi, and Praneeth Netrapalli. The step decay schedule: A near optimal, geometrically decaying learning rate procedure for least squares. *Neural Information Processing Systems (NeurIPS)*, 2019a. (Cited on pages 1 and 11)
- Rong Ge, Sham M. Kakade, Rahul Kidambi, and Praneeth Netrapalli. Rethinking learning rate schedules for stochastic optimization, 2019b. URL <https://openreview.net/forum?id=HJePy3RcF7>. (Cited on page 12)
- Priya Goya, Piotr Dollar, Ross Girshick, Pieter Noordhuis, Lukasz Wesolowski, Aapo Kyrola, Andrew Tulloch, Yangqing Jia, and Kaiming He. Accurate, large minibatch SGD: Training ImageNet in 1 hour. Technical report, Facebook, 2017. (Cited on page 2)

- Nicholas J. A. Harvey, Christopher Liaw, and Yaniv Plan Sikander Randhawa. Tight analyses for non-smooth stochastic gradient descent. *Annual Conference on Learning Theory (COLT)*, 2019. (Cited on page 12)
- Kaiming He, Xiangyu Zhang, Shaoqing Ren, and Jian Sun. Deep residual learning for image recognition. In *Proceedings of the IEEE conference on computer vision and pattern recognition*, 2016. (Cited on page 8)
- Jordan Hoffmann, Sebastian Borgeaud, Arthur Mensch, Elena Buchatskaya, Trevor Cai, Eliza Rutherford, Diego de las Casas, Lisa Anne Hendricks, Johannes Welbl, Aidan Clark, Tom Hennigan, Eric Noland, Katherine Millican, George van den Driessche, Bogdan Damoc, Aurelia Guy, Simon Osindero, Karen Simonyan, Erich Elsen, Oriol Vinyals, Jack William Rae, and Laurent Sifre. An empirical analysis of compute-optimal large language model training. In Alice H. Oh, Alekh Agarwal, Danielle Belgrave, and Kyunghyun Cho, editors, *Advances in Neural Information Processing Systems*, 2022. URL <https://openreview.net/forum?id=iBBcRUlOAPR>. (Cited on page 9)
- Gao Huang, Zhuang Liu, Laurens Van Der Maaten, and Kilian Q. Weinberger. Densely connected convolutional networks. In *2017 IEEE Conference on Computer Vision and Pattern Recognition (CVPR)*, pages 2261–2269, 2017. doi: 10.1109/CVPR.2017.243. (Cited on page 8)
- Maor Ivgi, Oliver Hinder, and Yair Carmon. DoG is SGD’s best friend: A parameter-free dynamic step size schedule. *The 40th International Conference on Machine Learning (ICML 2023)*, 2023. (Cited on page 5)
- Nikhil Iyer, V. Thejas, Nipun Kwatra, Ramachandran Ramjee, and Muthian Sivathanu. Lrtuner: A learning rate tuner for deep neural networks, 2021. (Cited on page 14)
- Prateek Jain, Dheeraj Nagaraj, and Praneeth Netrapalli. Making the last iterate of SGD information theoretically optimal. *Conference On Learning Theory (COLT)*, 2019. (Cited on pages 2, 4, and 12)
- Yuchen Jin, Tianyi Zhou, Liangyu Zhao, Yibo Zhu, Chuanxiong Guo, Marco Canini, and Arvind Krishnamurthy. Autolrs: Automatic learning-rate schedule by bayesian optimization on the fly. In *Proceedings of the Ninth International Conference on Learning Representations (ICLR 2021)*, 2021. (Cited on page 14)
- Ahmed Khaled, Konstantin Mishchenko, and Chi Jin. DoWG unleashed: An efficient universal parameter-free gradient descent method. *arXiv preprint arXiv:2305.16284*, 2023. (Cited on page 5)
- Chiheon Kim, Saehoon Kim, Jongmin Kim, Donghoon Lee, and Sungwoong Kim. Automated learning rate scheduler for large-batch training. *arXiv preprint arXiv:2107.05855*, 2021. (Cited on page 14)
- Diederik P. Kingma and Jimmy Ba. Adam: A method for stochastic optimization. In Yoshua Bengio and Yann LeCun, editors, *3rd International Conference on Learning Representations, ICLR 2015, San Diego, CA, USA, May 7-9, 2015, Conference Track Proceedings*, 2015. URL <http://arxiv.org/abs/1412.6980>. (Cited on pages 4 and 26)
- Alex Krizhevsky. Learning multiple layers of features from tiny images. Technical report, University of Toronto, 2009. (Cited on page 8)
- Alex Krizhevsky, Ilya Sutskever, and Geoffrey E Hinton. Imagenet classification with deep convolutional neural networks. In F. Pereira, C.J. Burges, L. Bottou, and K.Q. Weinberger, editors, *Advances in Neural Information Processing Systems*, volume 25. Curran Associates, Inc., 2012. (Cited on page 13)
- Simon Lacoste-Julien, Mark Schmidt, and Francis Bach. A simpler approach to obtaining an $O(1/t)$ convergence rate for the projected stochastic subgradient method, 2012. (Cited on page 11)
- Hunter Lang, Lin Xiao, and Pengchuan Zhang. Using statistics to automate stochastic optimization. In H. Wallach, H. Larochelle, A. Beygelzimer, F. d’Alché-Buc, E. Fox, and R. Garnett, editors, *Advances in Neural Information Processing Systems*, volume 32. Curran Associates, Inc., 2019. (Cited on page 14)

- Xiaoyu Li and Francesco Orabona. On the convergence of stochastic gradient descent with adaptive stepsizes. In *The 22nd international conference on artificial intelligence and statistics*, pages 983–992. PMLR, 2019. (Cited on page 13)
- Junhong Lin, Lorenzo Rosasco, and Ding-Xuan Zhou. Iterative regularization for learning with convex loss functions. *Journal of Machine Learning Research*, 17(77):1–38, 2016. URL <http://jmlr.org/papers/v17/15-115.html>. (Cited on pages 4 and 20)
- Yinhan Liu, Myle Ott, Naman Goyal, Jingfei Du, Mandar Joshi, Danqi Chen, Omer Levy, Mike Lewis, Luke Zettlemoyer, and Veselin Stoyanov. RoBERTa: A robustly optimized BERT pretraining approach. *arXiv preprint arXiv:1907.11692*, 2019. (Cited on page 8)
- Ilya Loshchilov and Frank Hutter. Decoupled weight decay regularization. *arXiv preprint arXiv:1711.05101*, 2017a. (Cited on page 4)
- Ilya Loshchilov and Frank Hutter. SGDR: Stochastic gradient descent with warm restarts, 2017b. (Cited on page 13)
- Maren Mahsereci and Philipp Hennig. Probabilistic line searches for stochastic optimization. *J. Mach. Learn. Res.*, 18(1):4262–4320, jan 2017. ISSN 1532-4435. (Cited on page 14)
- Brendan McMahan and Matthew Streeter. No-regret algorithms for unconstrained online convex optimization. *Advances in neural information processing systems*, 25, 2012. (Cited on page 5)
- Zakaria Mhammedi and Wouter M. Koolen. Lipschitz and comparator-norm adaptivity in online learning. In *Conference on Learning Theory*, pages 2858–2887. PMLR, 2020. (Cited on page 5)
- Maxim Naumov, Dheevatsa Mudigere, Hao-Jun Michael Shi, Jianyu Huang, Narayanan Sundaraman, Jongsoo Park, Xiaodong Wang, Udit Gupta, Carole-Jean Wu, Alisson G. Azzolini, Dmytro Dzhulgakov, Andrey Mallekovich, Ilia Cherniavskii, Yinghai Lu, Raghuraman Krishnamoorthi, Ansha Yu, Volodymyr Kondratenko, Stephanie Pereira, Xianjie Chen, Wenlin Chen, Vijay Rao, Bill Jia, Liang Xiong, and Misha Smelyanskiy. Deep learning recommendation model for personalization and recommendation systems. *CoRR*, 2019. (Cited on page 8)
- A. Nemirovski, A. Juditsky, G. Lan, and A. Shapiro. Robust stochastic approximation approach to stochastic programming. *SIAM Journal on Optimization*, 19(4):1574–1609, 2009. (Cited on page 11)
- Yurii Nesterov. *Lectures on Convex Optimization*. Springer Nature, 2018. (Cited on page 11)
- Francesco Orabona. Last iterate of SGD converges (even in unbounded domains), Aug 2020. URL <https://parameterfree.com/2020/08/07/last-iterate-of-sgd-converges-even-in-unbounded-domains/>. (Cited on pages 4 and 20)
- Francesco Orabona and Dávid Pál. Coin betting and parameter-free online learning. *Advances in Neural Information Processing Systems*, 29, 2016. (Cited on page 5)
- Rui Pan, Haishan Ye, and Tong Zhang. Eigencurve: Optimal learning rate schedule for SGD on quadratic objectives with skewed hessian spectrums. *International Conference on Learning Representations (ICLR)*, 2022. (Cited on pages 2 and 11)
- Fabian Pedregosa. Hyperparameter optimization with approximate gradient. In *International conference on machine learning*, pages 737–746. PMLR, 2016. (Cited on page 14)
- Georg Ch. Pflug. On the determination of the step size in stochastic quasigradient methods. *International Institute for Applied Systems Analysis (IIASA), Laxenburg, Austria*, 1983. (Cited on page 14)

- Georg Ch. Pflug. Adaptive stepsize control in stochastic approximation algorithms. In *Proceedings of 8th IFAC Symposium on Identification and System Parameter Estimation*, 1988. (Cited on page 14)
- Boris Polyak. New stochastic approximation type procedures. *Avtomatica i Telemekhanika*, 7:98–107, 01 1990. (Cited on pages 1 and 11)
- Alec Radford, Karthik Narasimhan, Tim Salimans, and Ilya Sutskever. Improving language understanding by generative pre-training. Technical report, OpenAI, 2019. (Cited on page 8)
- Colin Raffel, Noam Shazeer, Adam Roberts, Katherine Lee, Sharan Narang, Michael Matena, Yanqi Zhou, Wei Li, and Peter J. Liu. Exploring the limits of transfer learning with a unified text-to-text transformer. *Journal of Machine Learning Research*, 21(140):1–67, 2020. URL <http://jmlr.org/papers/v21/20-074.html>. (Cited on page 9)
- Alexander Rakhlin, Ohad Shamir, and Karthik Sridharan. Making gradient descent optimal for strongly convex stochastic optimization. In *Proceedings of the 29th International Conference on International Conference on Machine Learning, ICML'12*, 2012. (Cited on page 11)
- Sashank J. Reddi, Satyen Kale, and Sanjiv Kumar. On the convergence of Adam and beyond. In *Sixth International Conference on Learning Representations (ICLR), Vancouver, Canada, April 30 – May 3, 2018*, 2018. (Cited on page 4)
- Shaoqing Ren, Kaiming He, Ross Girshick, and Jian Sun. Faster R-CNN: Towards real-time object detection with region proposal networks. In *Advances in Neural Information Processing Systems*, volume 28. Curran Associates, Inc., 2015. (Cited on page 8)
- Herbert Robbins and Sutton Monro. A Stochastic Approximation Method. *The Annals of Mathematical Statistics*, 22(3):400 – 407, 1951. (Cited on page 10)
- David Ruppert. Efficient estimations from a slowly convergent robbins-monro process. *Technical Report, Cornell University*, 02 1988. (Cited on pages 1 and 11)
- Olga Russakovsky, Jia Deng, Hao Su, Jonathan Krause, Sanjeev Satheesh, Sean Ma, Zhiheng Huang, Andrej Karpathy, Aditya Khosla, Michael Bernstein, Alexander C. Berg, and Li Fei-Fei. ImageNet Large Scale Visual Recognition Challenge. *International Journal of Computer Vision (IJCV)*, 115(3), 2015. (Cited on page 8)
- Robin M Schmidt, Frank Schneider, and Philipp Hennig. Descending through a crowded valley - benchmarking deep learning optimizers. In Marina Meila and Tong Zhang, editors, *Proceedings of the 38th International Conference on Machine Learning*, volume 139 of *Proceedings of Machine Learning Research*, pages 9367–9376. PMLR, 18–24 Jul 2021. (Cited on page 13)
- Ohad Shamir and Tong Zhang. Stochastic gradient descent for non-smooth optimization: Convergence results and optimal averaging schemes. *International Conference on Machine Learning (ICML)*, 2013. (Cited on pages 11 and 12)
- Leslie N. Smith and Nicholay Topin. Super-convergence: Very fast training of residual networks using large learning rates, 2018. (Cited on page 13)
- Anuroop Sriram, Jure Zbontar, Tullie Murrell, Aaron Defazio, C. Lawrence Zitnick, Nafissa Yakubova, Florian Knoll, and Patricia Johnson. End-to-end variational networks for accelerated MRI reconstruction. In *International Conference on Medical Image Computing and Computer-Assisted Intervention*. Springer, 2020. (Cited on page 8)
- Matthew Streeter and H. Brendan McMahan. Less regret via online conditioning. *arXiv preprint arXiv:1002.4862*, 2010. (Cited on pages 4 and 13)

- Rachel Ward, Xiaoxia Wu, and Leon Bottou. Adagrad stepsizes: sharp convergence over nonconvex landscapes. In *International Conference on Machine Learning*, 2019. (Cited on page 13)
- Sam Wiseman and Alexander M. Rush. Sequence-to-sequence learning as beam-search optimization. In *Proceedings of the 2016 Conference on Empirical Methods in Natural Language Processing*. Association for Computational Linguistics, 2016. (Cited on pages 8 and 34)
- Xiaoxia Wu, Rachel Ward, and Léon Bottou. WNGrad: Learn the learning rate in gradient descent. *arXiv preprint arXiv:1803.02865*, 2020. (Cited on pages 1 and 13)
- Zhen Xu, Andrew M. Dai, Jonas Kemp, and Luke Metz. Learning an adaptive learning rate schedule. *arXiv preprint arXiv:1909.09712*, 2019. (Cited on page 14)
- Sergey Zagoruyko and Nikos Komodakis. Wide residual networks. In *Proceedings of the British Machine Vision Conference (BMVC)*, 2016. (Cited on page 8)
- Moslem Zamani and François Glineur. Exact convergence rate of the last iterate in subgradient methods. *arXiv preprint arXiv:2307.11134*, 2023. (Cited on pages 2, 4, and 12)
- Jure Zbontar, Florian Knoll, Anuroop Sriram, Matthew J. Muckley, Mary Bruno, Aaron Defazio, Marc Parente, Krzysztof J. Geras, Joe Katsnelson, Hersh Chandarana, et al. fastMRI: An open dataset and benchmarks for accelerated MRI. *arXiv preprint arXiv:1811.08839*, 2018. (Cited on page 8)
- Pengchuan Zhang, Hunter Lang, Qiang Liu, and Lin Xiao. Statistical adaptive stochastic gradient methods. *arXiv preprint arXiv:2002.10597*, 2020. (Cited on page 14)
- Zhiyu Zhang, Ashok Cutkosky, and Ioannis Paschalidis. PDE-based optimal strategy for unconstrained online learning. In *International Conference on Machine Learning*, pages 26085–26115. PMLR, 2022. (Cited on page 5)
- Yukun Zhu, Ryan Kiros, Rich Zemel, Ruslan Salakhutdinov, Raquel Urtasun, Antonio Torralba, and Sanja Fidler. Aligning books and movies: Towards story-like visual explanations by watching movies and reading books. In *Proceedings of the 2015 IEEE International Conference on Computer Vision (ICCV)*, 2015. (Cited on page 8)
- Martin Zinkevich. Online convex programming and generalized infinitesimal gradient ascent. In *Proceedings of the Twentieth International Conference on International Conference on Machine Learning*, pages 928–935, 2003. (Cited on pages 4 and 24)

Appendix A. All-Tail Summation Bound

In this section we develop some key Lemmas that underlie our results. The starting point of this development is the following result from Orabona (2020); Lin et al. (2016). We present the result and proof below for completeness, and then provide an improved version of the bound (Lemma 5) that is used to derive our analytical results.

A.1 Existing bound

Lemma 4 *Let $q_t \geq 0$, and let η_t be a positive non-increasing sequence. Then:*

$$\eta_T q_T \leq \frac{1}{T} \sum_{t=1}^T \eta_t q_t + \sum_{k=1}^{T-1} \frac{1}{k(k+1)} \sum_{t=k+1}^T \eta_t (q_t - q_k),$$

Proof We present below a version of the proof that's written to move the single inequality application in the whole proof to the last step. Define $S_k = \frac{1}{k} \sum_{t=T-k+1}^T \eta_t q_t$.

Then

$$\begin{aligned} kS_k &= (k+1)S_{k+1} - \eta_{T-k} q_{T-k} \\ &= kS_{k+1} + S_{k+1} - \eta_{T-k} q_{T-k} \\ &= kS_{k+1} + \frac{1}{k+1} \sum_{t=T-k}^T (\eta_t q_t - \eta_{T-k} q_{T-k}). \end{aligned}$$

Dividing through by k :

$$S_k = S_{k+1} + \frac{1}{k(k+1)} \sum_{t=T-k}^T (\eta_t q_t - \eta_{T-k} q_{T-k}).$$

Unrolling, we have:

$$S_1 = S_T + \sum_{k=1}^{T-1} \frac{1}{k(k+1)} \sum_{t=T-k}^T (\eta_t q_t - \eta_{T-k} q_{T-k}).$$

Now we use $S_1 = \eta_T q_T$. Note that the first entry in that sum is zero so we may shift the indexing to start at $t = T - k + 1$. Giving:

$$\begin{aligned} \eta_T q_T &= S_T + \sum_{k=1}^{T-1} \frac{1}{k(k+1)} \sum_{t=T-k+1}^T (\eta_t q_t - \eta_{T-k} q_{T-k}) \\ &\leq S_T + \sum_{k=1}^{T-1} \frac{1}{k(k+1)} \sum_{t=T-k+1}^T \eta_t (q_t - q_{T-k}). \end{aligned}$$

Where the final step uses the fact that η_t is decreasing. Plugging in the definition of S_T , and substituting $k = T - k$ to simplify gives the result. ■

A.2 Improved expression

Lemma 5 *Let q_t be any sequence, and let w_t be a positive sequence. Then:*

$$\begin{aligned} q_T &= \frac{1}{\sum_{t=1}^T w_t} \sum_{t=1}^T w_t q_t + \sum_{k=1}^{T-1} \frac{w_k}{\sum_{t=k+1}^T w_t} \left(\frac{1}{\sum_{t=k}^T w_t} \sum_{t=k}^T w_t (q_t - q_k) \right) \\ &= \frac{1}{w_{1:T}} \sum_{t=1}^T w_t q_t + \sum_{k=1}^{T-1} \left(\frac{1}{w_{k+1:T}} - \frac{1}{w_{k:T}} \right) \sum_{t=k}^T w_t (q_t - q_k). \end{aligned}$$

Proof Define

$$S_k = \frac{1}{\sum_{t=T-k+1}^T w_t} \sum_{t=T-k+1}^T w_t q_t.$$

Note that with this definition:

$$S_1 = \frac{1}{\sum_{t=1}^T w_t} \sum_{t=1}^T w_t q_t = q_T,$$

and S_T is the full sum:

$$S_T = \frac{1}{\sum_{t=1}^T w_t} \sum_{t=1}^T w_t q_t.$$

The difference from the weighting used in the the Lemma above: we normalized by the sum of the step sizes rather than k . We get the following expansion:

$$\begin{aligned} \left(\sum_{t=T-k+1}^T w_t \right) S_k &= \sum_{t=T-k+1}^T w_t q_t \\ &= \sum_{t=T-k}^T w_t q_t - w_{T-k} q_{T-k} \\ &= \left(\sum_{t=T-k}^T w_t \right) S_{k+1} - w_{T-k} q_{T-k} \\ &= \left(\sum_{t=T-k+1}^T w_t \right) S_{k+1} + (w_{T-k} S_{k+1} - w_{T-k} q_{T-k}). \end{aligned}$$

So dividing through by $\sum_{t=T-k+1}^T w_t$:

$$S_k = S_{k+1} + \frac{w_{T-k}}{\sum_{t=T-k+1}^T w_t} (S_{k+1} - q_{T-k}).$$

Unrolling

$$S_1 = S_T + \sum_{k=1}^{T-1} \frac{w_{T-k}}{\sum_{t=T-k+1}^T w_t} (S_{k+1} - q_{T-k}).$$

Note that, plugging in S_{k+1} :

$$\begin{aligned} S_{k+1} - q_{T-k} &= \frac{1}{\sum_{t=T-k}^T w_t} \sum_{t=T-k}^T w_t q_t - q_{T-k} \\ &= \frac{1}{\sum_{t=T-k}^T w_t} \sum_{t=T-k}^T w_t (q_t - q_{T-k}). \end{aligned}$$

So we have:

$$q_T = \frac{1}{\sum_{t=1}^T w_t} \sum_{t=1}^T w_t q_t + \sum_{k=1}^{T-1} \frac{w_{T-k}}{\sum_{t=T-k+1}^T w_t} \left(\frac{1}{\sum_{t=T-k}^T w_t} \sum_{t=T-k}^T w_t (q_t - q_{T-k}) \right).$$

Finally, we make the simple change of variables $k \rightarrow T - k$ to yield the result. \blacksquare

Remark 6 We will typically use this result by setting $q_t = f(x_t) - f_*$ in order to bound $q_T = f(x_T) - f_*$. By using a weighting sequence w_t elsewhere, we are able to remove the w_T weight from in front of the q_T term (in contrast to Lemma 4). This is crucial, as we want to be able to analyze the situation in which w_t drops extremely small near the end, and yet still bound $q_T = f(x_T) - f_*$, but if q_T is weighted by w_T we will get very loose bounds when w_T is small. Notice also that we have an equality instead of an inequality, and we have not had to impose the requirement that w be a non-increasing sequence.

Appendix B. Proof of Theorem 1

Before proving Theorem 1, we need the following important Lemma:

Lemma 7 Suppose z_1, \dots, z_T is an arbitrary sequence of vectors. Let w_1, \dots, w_T be an arbitrary sequence of positive numbers. Define the sequence x_1, \dots, x_T recursively by $x_1 = z_1$ and:

$$x_t = w_{t:T} \left(\frac{z_t}{w_{1:T}} + \sum_{p=1}^{t-1} x_p \left(\frac{1}{w_{p+1:T}} - \frac{1}{w_{p:T}} \right) \right).$$

Suppose g_t are random variables. with $\mathbb{E}[g_t | x_1, \dots, x_t] \in \partial f(x_t)$ for some convex f . Then:

$$\mathbb{E}[f(x_T) - f(u)] \leq \mathbb{E} \left[\frac{1}{w_{1:T}} \sum_{t=1}^T w_t \langle g_t, z_t - u \rangle \right].$$

Proof Let us set $q_t = f(x_t) - f(u)$. Then we have $\mathbb{E}[q_t] \leq \mathbb{E}[\langle g_t, x_t - u \rangle]$ and $\mathbb{E}[q_t - q_k] \leq \mathbb{E}[\langle g_t, x_t - x_k \rangle]$. Then, Lemma 5 implies:

$$\mathbb{E}[q_T] \leq \mathbb{E} \left[\frac{1}{w_{1:T}} \sum_{t=1}^T w_t \langle g_t, x_t - u \rangle + \sum_{k=1}^{T-1} \left(\frac{1}{w_{k+1:T}} - \frac{1}{w_{k:T}} \right) \sum_{t=k}^T w_t \langle g_t, x_t - x_k \rangle \right].$$

Now, let us find the coefficient of $\langle g_t, x_t \rangle$ in the above expression. This is:

$$\begin{aligned} & \frac{w_t}{w_{1:T}} + \left[\sum_{k=1}^t \left(\frac{1}{w_{k+1:T}} - \frac{1}{w_{k:T}} \right) w_t \right] - w_t \left(\frac{1}{w_{t+1:T}} - \frac{1}{w_{t:T}} \right) \\ &= \frac{w_t}{w_{1:T}} + \sum_{k=1}^{t-1} \left(\frac{1}{w_{k+1:T}} - \frac{1}{w_{k:T}} \right) w_t \\ &= \frac{w_t}{w_{t:T}}. \end{aligned}$$

Next, for $p < t$, the coefficient of $\langle g_t, x_p \rangle$ is:

$$- \left(\frac{1}{w_{p+1:T}} - \frac{1}{w_{p:T}} \right) w_t.$$

And for $p > t$, the coefficient of $\langle g_t, x_p \rangle$ is zero. Finally the coefficient of $\langle g_t, u \rangle$ is $-\frac{w_t}{w_{1:T}}$.

Putting this all together, we can rearrange the expression as follows:

$$\begin{aligned} \mathbb{E}[q_T] &\leq \mathbb{E} \left[\sum_{t=1}^T \left\langle g_t, \frac{w_t}{w_{t:T}} x_t - \left(\frac{w_t u}{w_{1:T}} + \sum_{p=1}^{t-1} w_t x_p \left(\frac{1}{w_{p+1:T}} - \frac{1}{w_{p:T}} \right) \right) \right\rangle \right] \\ &= \mathbb{E} \left[\sum_{t=1}^T \left\langle \frac{w_t}{w_{t:T}} g_t, x_t - w_{t:T} \left(\frac{u}{w_{1:T}} + \sum_{p=1}^{t-1} x_p \left(\frac{1}{w_{p+1:T}} - \frac{1}{w_{p:T}} \right) \right) \right\rangle \right]. \end{aligned}$$

Now, given an arbitrary sequence z_1, \dots, z_T , define x_t recursively by:

$$x_t = w_{t:T} \left(\frac{z_t}{w_{1:T}} + \sum_{p=1}^{t-1} x_p \left(\frac{1}{w_{p+1:T}} - \frac{1}{w_{p:T}} \right) \right).$$

Then we have:

$$\begin{aligned} \mathbb{E}[q_T] &\leq \mathbb{E} \left[\sum_{t=1}^T \left\langle \frac{w_t}{w_{t:T}} g_t, x_t - w_{t:T} \left(\frac{u}{w_{1:T}} + \sum_{p=1}^{t-1} x_p \left(\frac{1}{w_{p+1:T}} - \frac{1}{w_{p:T}} \right) \right) \right\rangle \right] \\ &= \mathbb{E} \left[\sum_{t=1}^T \frac{w_t}{w_{1:T}} \langle g_t, z_t - u \rangle \right]. \end{aligned}$$

■

Now, we are finally ready to prove Theorem 1:

Theorem 1 *Suppose z_1, \dots, z_T is some arbitrary sequence of vectors. Let w_1, \dots, w_T be an arbitrary sequence of non-negative numbers. Recall that we define $\Delta_t = z_{t+1} - z_t$ and $x_1 = z_1$. For $t \geq 1$, suppose x_{t+1} satisfies:*

$$x_{t+1} = x_t + \frac{w_{t+1:T}}{w_{1:T}} \Delta_t,$$

then for any u :

$$\mathbb{E}[f(x_T) - f(u)] \leq \mathbb{E} \left[\sum_{t=1}^T \frac{1}{w_{1:T}} \langle w_t \cdot g_t, z_t - u \rangle \right].$$

Proof Let's define $\hat{x}_1 = z_1$ and recursively set:

$$\hat{x}_t = w_{t:T} \left(\frac{z_t}{w_{1:T}} + \sum_{p=1}^{t-1} \hat{x}_p \left(\frac{1}{w_{p+1:T}} - \frac{1}{w_{p:T}} \right) \right).$$

Then, Lemma 7 shows that $\mathbb{E}[f(\hat{x}_T) - f(u)] \leq \mathbb{E} \left[\frac{1}{w_{1:T}} \sum_{t=1}^T w_t \langle g_t, z_t - u \rangle \right]$. So, it suffices to show that $x_t = \hat{x}_t$ for all t . In turn, since $\hat{x}_1 = z_1 = x_1$, it suffices to show $\hat{x}_{t+1} - \hat{x}_t = \frac{w_{t+1:T}}{w_{1:T}} \Delta_t = x_{t+1} - x_t$ for all t .

To this end, let's do some calculation. First:

$$\begin{aligned} \hat{x}_t &= \frac{w_t}{w_{t:T}} \hat{x}_t + \frac{w_{t+1:T}}{w_{t:T}} \hat{x}_t \\ &= \frac{w_t}{w_{t:T}} \hat{x}_t + w_{t+t:T} \left(\frac{z_t}{w_{1:T}} + \sum_{p=1}^{t-1} \hat{x}_p \left(\frac{1}{w_{p+1:T}} - \frac{1}{w_{p:T}} \right) \right). \end{aligned}$$

With this expression, we have:

$$\begin{aligned}
 \hat{x}_{t+1} - \hat{x}_t &= \hat{x}_{t+1} - w_{t+1:T} \left(\frac{z_{t+1}}{w_{1:T}} + \sum_{p=1}^t x_p \left(\frac{1}{w_{p+1:T}} - \frac{1}{w_{p:T}} \right) \right) - \frac{w_t}{w_{t:T}} \hat{x}_t \\
 &= w_{t+1:T} \left(\frac{z_{t+1}}{w_{1:T}} + \sum_{p=1}^t \hat{x}_p \left(\frac{1}{w_{p+1:T}} - \frac{1}{w_{p:T}} \right) \right) \\
 &\quad - w_{t+1:T} \left(\frac{z_t}{w_{1:T}} + \sum_{p=1}^{t-1} x_p \left(\frac{1}{w_{p+1:T}} - \frac{1}{w_{p:T}} \right) \right) - \frac{w_t}{w_{t:T}} \hat{x}_t \\
 &= \frac{w_{t+1:T}(z_{t+1} - z_t)}{w_{1:T}} + w_{t+1:T} \hat{x}_t \left(\frac{1}{w_{t+1:T}} - \frac{1}{w_{t:T}} \right) - \frac{w_t}{w_{t:T}} \hat{x}_t \\
 &= \frac{w_{t+1:T}}{w_{1:T}} \Delta_t + \hat{x}_t \left(1 - \frac{w_{t+1:T} + w_t}{w_{t:T}} \right) \\
 &= \frac{w_{t+1:T}}{w_{1:T}} \Delta_t.
 \end{aligned}$$

■

Appendix C. Proof of Theorem 3

Theorem 3 Suppose that $x_{t+1} = x_t - \eta_t g_t$ with $\eta_t = \frac{w_t w_{t+1:T}}{w_{1:T}}$. Then we have:

$$\mathbb{E}[f(x_T) - f(u)] \leq \mathbb{E} \left[\frac{1}{2 \cdot w_{1:T}} \left(D^2 + \sum_{t=1}^T w_t^2 \|g_t\|^2 \right) \right]. \quad (2)$$

Moreover, for a fixed sequence $\|g_1\|^2, \dots, \|g_T\|^2$, the value of $\frac{1}{2 \cdot w_{1:T}} (D^2 + \sum_{t=1}^T w_t^2 \|g_t\|^2)$ is minimized by setting:

$$w_t = \|g_t\|^{-2} \frac{D}{\sqrt{\sum_{p=1}^T \|g_p\|^{-2}}}.$$

Proof First, observe that with $\Delta_t = -w_t \eta_t$, we have $x_{t+1} = x_t + \frac{w_{t+1:T}}{w_{1:T}} \Delta_t$. Therefore with $z_1 = x_1$ and $z_{t+1} = z_t + \Delta_t$, Theorem 1 implies:

$$\mathbb{E}[f(x_T) - f(u)] \leq \mathbb{E} \left[\frac{1}{w_{1:T}} \sum_{t=1}^T \langle w_t g_t, z_t - u \rangle \right].$$

Next, observe that z_t is simply online gradient descent with learning rate 1 acting on the loss vectors $w_t z_t$. Standard analysis (Zinkevich, 2003) shows:

$$\sum_{t=1}^T \langle w_t g_t, z_t - u \rangle = \frac{\|z_1 - u\|^2}{2} - \frac{\|z_{T+1} - u\|^2}{2} + \sum_{t=1}^T \frac{w_t^2 \|g_t\|^2}{2}.$$

This immediately implies the first part of the Theorem. Next, we need to solve for the minimizing values of w_t . To do this, we take the logarithm of the expression $\frac{1}{2w_{1:T}} \left(\|x_1 - u\|^2 + \sum_{t=1}^T w_t^2 \|g_t\|^2 \right)$ and differentiate:

$$\frac{\partial}{\partial w_k} \log \left[\frac{1}{2w_{1:T}} \left(\|x_1 - u\|^2 + \sum_{t=1}^T w_t^2 \|g_t\|^2 \right) \right] = \frac{2w_k \|g_k\|^2}{\|x_1 - u\|^2 + \sum_{t=1}^T w_t^2 \|g_t\|^2} - \frac{1}{w_{1:T}}.$$

We set this equal to zero to solve for the optimal w_k :

$$w_k = \|g_k\|^{-2} \frac{\|x_1 - u\|^2 + \sum_{t=1}^T w_t^2 \|g_t\|^2}{2w_{1:T}} \triangleq \lambda \|g_k\|^{-2},$$

where we have defined $\lambda = \frac{\|x_1 - u\|^2 + \sum_{t=1}^T w_t^2 \|g_t\|^2}{2w_{1:T}}$, which does not depend on k . That is, the optimal w_k value is proportional to $\|g_k\|^{-2}$. With this expression, we have:

$$\begin{aligned} \sum_{t=1}^T w_t^2 \|g_t\|^2 &= \lambda^2 \sum_{t=1}^T \|g_t\|^{-2} \\ w_{1:T} &= \lambda \sum_{t=1}^T \|g_t\|^{-2}. \end{aligned}$$

So, let us now solve for λ by plugging in these values:

$$\begin{aligned} \lambda &= \frac{\|x_1 - u\|^2 + \sum_{t=1}^T w_t^2 \|g_t\|^2}{2w_{1:T}} \\ \lambda &= \frac{\|x_1 - u\|^2 + \lambda^2 \sum_{t=1}^T \|g_t\|^{-2}}{2\lambda \sum_{t=1}^T \|g_t\|^{-2}} \\ \lambda &= \frac{\|x_1 - u\|^2}{2\lambda \sum_{t=1}^T \|g_t\|^{-2}} + \frac{\lambda}{2} \\ \lambda &= \frac{\|x_1 - u\|}{\sqrt{\sum_{t=1}^T \|g_t\|^{-2}}}. \end{aligned}$$

This in turn implies the claimed optimal value for w_k . ■

Appendix D. Proof of Theorem 9

Proof First, observe that for any solution to the desired identity $\eta_t = \frac{w_t w_{t+1:T}}{w_{1:T}}$, replacing w with $c \cdot w$ for some constant c will yield a solution for η replaced with $c \cdot \eta$. Thus, it suffices to consider the possibility that $\max_t \eta_t = 1$.

The intuition for the rest of the proof is the following: Given the value for w_1 , we can solve for $w_{2:T}$ using the equation $\frac{w_1 w_{2:T}}{w_1 + w_{2:T}} = \eta_1$. This in turn provides us with the value of $w_{1:T}$. Now, given $w_{k:T}$ for any k we can solve for w_k using the equation $\eta_k = \frac{w_k w_{k+1:T}}{w_{1:T}} = \frac{w_k (w_{k:T} - w_k)}{w_{1:T}}$. Thus we may recursively compute all the values of w . Each of these steps requires solving a quadratic equation. We simply choose an initial w_1 so as to ensure that all the following quadratic equations have non-negative real roots.

Specifically, set $w_1 = \frac{2^{2T} + \sqrt{2^{4T} - 4\eta_1}}{2}$ and define $s_1 = 2^{2T}$. Then, recursively define for $t = 2, \dots, T-1$:

$$\begin{aligned} s_t &= s_{t-1} - w_{t-1} \\ w_t &= \frac{s_t - \sqrt{s_t^2 - 4s_1\eta_t}}{2} \end{aligned}$$

and set $w_T = s_T = s_{T-1} - w_{T-1}$. Notice that these choices satisfy:

$$w_t^2 - s_t w_t + s_1 \eta_t = 0$$

so that if we could establish (1) that all $w_t \geq 0$ and (2) $s_t = w_{t:T}$, then we would have:

$$\begin{aligned} \frac{w_t w_{t+1:T}}{w_{1:T}} &= \frac{w_t (w_{t:T} - w_t)}{w_{1:T}} \\ &= \frac{w_t (s_t - w_t)}{s_1} \\ &= \frac{s_t w_t - w_t^2}{s_1} \\ &= \eta_t \end{aligned}$$

as desired.

Let us first prove (1): all $w_t \geq 0$. For $t \leq T - 1$, this will hold if $s_t^2 - 4s_1\eta_t > 0$. To establish this, we will first show that $s_t \geq \frac{s_1}{2^{t-1}}$ for all $t \leq T - 1$. If this holds, then we have:

$$s_t^2 \geq \frac{s_1^2}{2^{2t-2}} \geq \frac{s_1 2^{2T}}{2^{2t-2}} \geq 4s_1 \geq 4s_1\eta_t$$

for $t \leq T - 1$, where we have used our assumption $\eta_t \leq 1$.

So, we now establish $s_t \geq \frac{s_1}{2^{t-1}}$ by induction for $t \leq T - 1$. The statement is clear for $t = 1$. Suppose it holds for all $t \leq k$ for some $k \leq T - 2$. Then we have:

$$\begin{aligned} s_{k+1} &= s_k - w_k \\ &= \frac{s_k + \sqrt{s_k^2 - 4s_1\eta_k}}{2} \\ &\geq \frac{s_k}{2} \\ &\geq \frac{s_1}{2^{k-1+1}}, \end{aligned}$$

which establishes the claim. Therefore for $t \leq T - 1$, w_t are non-negative real numbers. Finally, we have:

$$w_{T-1} = \frac{s_{T-1} + \sqrt{s_{T-1}^2 - 4s_1\eta_{T-1}}}{2} \leq s_{T-1},$$

so that $w_T = s_T = s_{T-1} - w_{T-1} \geq 0$. Thus $w_t \geq 0$ for all t .

Next, to show (2): $s_t = w_{t:T}$. This is nearly immediate. By definition we have $w_T = s_T$. Suppose $s_k = w_{k:T}$ for some $k \geq 2$. Then $s_t = s_{t-1} - w_{t-1}$ so that $s_{t-1} = s_t + w_{t-1} = w_{t-1:T}$. Thus by induction we have $s_t = w_{t:T}$ for all t , which is the last thing we needed to show. \blacksquare

Appendix E. Schedules for Per-Coordinate Updates

Many popular optimization algorithms in use today like Adam (Kingma and Ba, 2015) and its variants employ *per-coordinate* updates: the update Δ_t is not proportional to the gradient g_t but instead scales each coordinate of g_t by an adaptively chosen value. In this section we propose an approximately optimal schedule for such methods.

Theorem 8 Suppose $\Delta_t = z_{t+1} - z_t = -w_t \cdot (\eta_t \odot g_t)$ where $\eta_t \in \mathbb{R}^d$ is a vector of learning rates and \odot indicates coordinate-wise product. Set $x_{t+1} = x_t - \frac{w_{t+1:T}}{w_{1:T}} \Delta_t$. Define the quantity R by:

$$R = \sqrt{\sum_{t=1}^T \sum_{i=1}^d \frac{(z_{t,i} - u_i)^2 - (z_{t+1,i} - u_i)^2}{\eta_{t,i}}}$$

Then we have:

$$\mathbb{E}[f(x_T) - f(u)] \leq \mathbb{E} \left[\frac{1}{w_{1:T}} \left(\frac{R^2}{2} + \sum_{t=1}^T w_t^2 \sum_{i=1}^d \eta_{t,i} g_{t,i}^2 \right) \right].$$

Moreover, for any given fixed values for R and $g_{t,i}^2$, the expression $\frac{1}{w_{1:T}} \left(\frac{R^2}{2} + \sum_{t=1}^T w_t^2 \sum_{i=1}^d \eta_{t,i} g_{t,i}^2 \right)$ is minimized by setting w_t as below:

$$w_t = \frac{R}{\sqrt{\sum_{t=1}^T \left(\sum_{i=1}^d \eta_{t,i} g_{t,i}^2 \right)^{-1}}} \cdot \left(\sum_{i=1}^d \eta_{t,i} g_{t,i}^2 \right)^{-1}.$$

As an example of how to use this result, let us suppose we are employing the Adam optimizer, and let us also ignore the presence of momentum when computing the weights (so really, these will be the weights for the RMSProp optimizer). In this case, $\eta_{t,i} \propto \frac{1}{\sqrt{v_{t,i}}}$ where $v_{t,i}$ is the exponential average of the squared gradients. Thus, we get:

$$w_t = \lambda \left(\sum_{i=1}^d \frac{g_{t,i}^2}{\sqrt{v_{t,i}}} \right)^{-1}$$

for some λ . Then, we use a learning rate schedule of $\frac{w_t w_{t+1:T}}{w_{1:T}}$.

That is, the corresponding procedure to Algorithm 1 is given by Algorithm 2:

Algorithm 2 Schedule Refinement for Adam

- 1: **Input:** $G = \left(G_t = \sum_{i=1}^d \frac{g_{t,i}^2}{\sqrt{v_{t,i}}} \right)$ length T sequence of weighted gradient norms from Adam optimizer, smoothing hyper-parameter $\tau > 0$
- 2: $\hat{G} = \text{median_filter}(G, \text{filter_width} = \tau T, \text{padding} = (\text{nearest}, \text{reflect}))$
- 3: Define $w_t = \hat{G}_t^{-1}$
- 4: For each t , let:
- 5:

$$\eta_t = w_t \sum_{p=t+1}^T w_p$$

- 6: Return normalized schedule $\eta / \max(\eta)$
-

In practice, however, recording the value $w_t \propto \left(\sum_{i=1}^d \frac{g_{t,i}^2}{\sqrt{v_{t,i}}} \right)^{-1}$ may be difficult (for example, in Pytorch, the Adam implementation is primarily C code rather than Python, which makes it substantially more involved to modify). However, by inspecting the formula for w_t , we can see that it is likely to be an interpolation between the $1/\|g_t\|_2^2$ and $1/\|g_t\|_1$ (the L1 norm is not squared). The intuition behind this is that if $v_{t,i}$ has a minimum value of $|g_{t,i}|$. With this minimum value, $w_t \propto 1/\|g_t\|_1$. On the other hand if all $v_{t,i}$ are the same constant, then $w_t \propto 1/\|g_t\|_2^2$. In practice we expect behavior closer to the first case and recommend using $w_t \propto 1/\|g_t\|_1$.

Proof [proof of Theorem 8] By standard online gradient descent analysis, we have:

$$\begin{aligned} \langle w_t \cdot g_t, z_t - u \rangle &= \sum_{i=1}^d w_t g_{t,i} (z_{t,i} - u_i) \\ &= \sum_{i=1}^d \frac{(z_{t,i} - u_i)^2}{2\eta_{t,i}} - \frac{(z_{t+1,i} - u_i)^2}{2\eta_{t,i}} + \frac{\eta_{t,i}}{2} w_t^2 g_{t,i}^2. \end{aligned}$$

Summing this over t from 1 to T , we get

$$\begin{aligned} \sum_{t=1}^T \langle w_t \cdot g_t, z_t - u \rangle &= \sum_{t=1}^T \sum_{i=1}^d \frac{(z_{t,i} - u_i)^2}{2\eta_{t,i}} - \frac{(z_{t+1,i} - u_i)^2}{2\eta_{t,i}} + \sum_{t=1}^T w_t^2 \sum_{i=1}^d \frac{\eta_{t,i} g_{t,i}^2}{2} \\ &= \frac{R^2}{2} + \sum_{t=1}^T \frac{w_t^2}{2} \sum_{i=1}^d \eta_{t,i} g_{t,i}^2. \end{aligned}$$

The first part of the result now follows from Theorem 1.

Next, we again take the logarithm, differentiate and set equal to zero:

$$\begin{aligned} 0 &= \frac{\partial}{\partial w_k} \log \left(\frac{1}{w_{1:T}} \left(\frac{R^2}{2} + \sum_{t=1}^T \frac{w_t^2}{2} \sum_{i=1}^d \eta_{t,i} g_{t,i}^2 \right) \right) \\ &= \frac{2w_k \sum_{i=1}^d \eta_{k,i}^2 g_{k,i}^2}{R^2 + \sum_{t=1}^T w_t^2 \sum_{i=1}^d \eta_{t,i} g_{t,i}^2} - \frac{1}{w_{1:T}}. \end{aligned}$$

Rearranging, we obtain

$$\begin{aligned} w_k &= \frac{\left(\sum_{i=1}^d \eta_{k,i}^2 g_{k,i}^2 \right)^{-1} \left(R^2 + \sum_{t=1}^T w_t^2 \sum_{i=1}^d \eta_{t,i} g_{t,i}^2 \right)}{2w_{1:T}} \\ &\triangleq \lambda \left(\sum_{i=1}^d \eta_{k,i} g_{k,i}^2 \right)^{-1}, \end{aligned}$$

where we have collected the non k -dependent terms into $\lambda = \frac{R^2 + \sum_{t=1}^T w_t^2 \sum_{i=1}^d \eta_{t,i} g_{t,i}^2}{2w_{1:T}}$. Now we solve for λ :

$$\begin{aligned} \lambda &= \frac{R^2 + \sum_{t=1}^T w_t^2 \sum_{i=1}^d \eta_{t,i} g_{t,i}^2}{2w_{1:T}} \\ &= \frac{R^2 + \lambda^2 \sum_{t=1}^T \left(\sum_{i=1}^d \eta_{t,i} g_{t,i}^2 \right)^{-1}}{2\lambda \sum_{t=1}^T \left(\sum_{i=1}^d \eta_{t,i} g_{t,i}^2 \right)^{-1}} \\ &= \frac{R^2}{2\lambda \sum_{t=1}^T \left(\sum_{i=1}^d \eta_{t,i} g_{t,i}^2 \right)^{-1}} + \frac{\lambda}{2} \\ &= \frac{R}{\sqrt{\sum_{t=1}^T \left(\sum_{i=1}^d \eta_{t,i} g_{t,i}^2 \right)^{-1}}}. \end{aligned}$$

Putting $w_t = \lambda \left(\sum_{i=1}^d \eta_{t,i} g_{t,i}^2 \right)^{-1}$ completes the proof. \blacksquare

Appendix F. Explicit bounds for arbitrary schedules

Section 2 develops a framework that suggests using learning rates of the form $\eta_t = \frac{w_t w_{t+1:T}}{w_{1:T}}$ and in Theorem 3 we provided a simple closed-form solution for the optimal values of w_t . Given this apparently restricted form of η_t , it is natural to ask if this restriction is real: that is, can *every* schedule $\eta_1, \dots, \eta_{T-1}$ be represented using some weights w_t ? Theorem 9 shows that the answer is “yes”:

Theorem 9 Let $\eta_1, \dots, \eta_{T-1}$ be a sequence of non-negative numbers with $\eta_1 \geq 0$. Then there is a sequence of non-negative weights w_1, \dots, w_T such that $\eta_t = \frac{w_t w_{t+1:T}}{w_{1:T}}$ for all t .

This Theorem shows that by optimizing the weights w_t , we are in some sense also solving for the optimal learning rate η_t . However, notice that the reverse is not true: any given schedule η_t can be represented by a number of different weights w_t , and these weights give rise to different bounds using Theorem 1. The proof of Theorem 9 works by constructing a particular set of weights w_t , but these may not be the best weights in terms of providing the tightest convergence bound for the given η_t .

Although Theorem 9 shows that the learning rate representation of Theorem 3 indeed covers all possible schedules, it does not provide a user-friendly way to analyze the convergence of an arbitrary schedule. In this section, we provide an alternative analysis that fills this gap.

This approach is closer to previous final-iterate analysis techniques: we bound the final iterate in terms of the average iterate, plus an additional *error* term. This bound is strictly looser than those of Theorems 1 and 3 in the constant factors, but provides a convenient way to analyze arbitrary schedules. The bound is presented in Theorem 10 below.

Theorem 10 Suppose that f is convex and let x_t be given by SGD with learning rates η_t : $x_{t+1} = x_t - \eta_t g_t$. Then for the last iterate x_T we have:

$$\begin{aligned} \mathbb{E}[f(x_T) - f(u)] &\leq \mathbb{E} \left[\frac{1}{2 \sum_{t=1}^T \eta_t} D^2 + \frac{1}{2 \sum_{t=1}^T \eta_t} \sum_{t=1}^T \eta_t^2 \|g_t\|^2 \right] \\ &+ \mathbb{E} \left[\frac{1}{2} \sum_{k=1}^{T-1} \frac{\eta_k}{\sum_{t=k+1}^T \eta_t} \left(\frac{1}{\sum_{t=k}^T \eta_t} \sum_{t=k}^T \eta_t^2 \|g_t\|^2 \right) \right]. \end{aligned} \quad (5)$$

Optimizing this bound with respect to the step-size sequence produces schedules that are visually indistinguishable from those of the regret based approach described in Section 2.1 for large T .

To prove Theorem 10, we will need to control quantities like:

$$\sum_{t=k}^T \eta_t (q_t - q_k) = f(x_t) - f(x_k).$$

This can be bounded by the usual suboptimality inequality for SGD/GD methods, which holds for any u :

$$\sum_{t=k}^T \eta_t [f(x_t) - f(u)] \leq \frac{1}{2} \|x_k - u\|^2 + \frac{1}{2} \sum_{t=k}^T \eta_t^2 \|g_t\|^2,$$

Setting $u = x_k$ yields:

$$\sum_{t=k}^T \eta_t [q_t - q_k] \leq \frac{1}{2} \sum_{t=k}^T \eta_t^2 \|g_t\|^2.$$

We can use this in our Lemma 5 to obtain the following result:

Corollary 11

$$q_T = \frac{1}{\sum_{t=1}^T \eta_t} \sum_{t=1}^T \eta_t q_t + \frac{1}{2} \sum_{k=1}^{T-1} \frac{\eta_k}{\sum_{t=k+1}^T \eta_t} \left(\frac{1}{\sum_{t=k}^T \eta_t} \sum_{t=k}^T \eta_t^2 \|g_t\|^2 \right).$$

Now, we are ready to prove Theorem 10.

Theorem 10 Suppose that f is convex and let x_t be given by SGD with learning rates η_t : $x_{t+1} = x_t - \eta_t g_t$. Then for the last iterate x_T we have:

$$\begin{aligned} \mathbb{E}[f(x_T) - f(u)] &\leq \mathbb{E} \left[\frac{1}{2 \sum_{t=1}^T \eta_t} D^2 + \frac{1}{2 \sum_{t=1}^T \eta_t} \sum_{t=1}^T \eta_t^2 \|g_t\|^2 \right] \\ &+ \mathbb{E} \left[\frac{1}{2} \sum_{k=1}^{T-1} \frac{\eta_k}{\sum_{t=k+1}^T \eta_t} \left(\frac{1}{\sum_{t=k}^T \eta_t} \sum_{t=k}^T \eta_t^2 \|g_t\|^2 \right) \right]. \end{aligned} \quad (5)$$

Proof Following the standard convergence bound approach:

$$\begin{aligned} \|x_{t+1} - u\|^2 &= \|x_t - \eta_t g_t - u\|^2 \\ &= \|x_t - u\|^2 - 2\eta_t \langle g_t, x_t - u \rangle + \eta_t^2 \|g_t\|^2 \\ &\leq \|x_t - u\|^2 - 2\eta_t [f(x_t) - f(u)] + \eta_t^2 \|g_t\|^2. \end{aligned}$$

Summing over t and telescoping gives:

$$\sum_{t=1}^T \eta_t [f(x_t) - f(u)] \leq \frac{1}{2} D^2 + \sum_{t=1}^T \eta_t^2 \|g_t\|^2.$$

Then divide through by $\sum_{t=1}^T \eta_t$:

$$\frac{1}{\sum_{t=1}^T \eta_t} \sum_{t=1}^T \eta_t [f(x_t) - f_*] \leq \frac{1}{2 \sum_{t=1}^T \eta_t} D^2 + \frac{1}{2 \sum_{t=1}^T \eta_t} \sum_{t=1}^T \eta_t^2 \|g_t\|^2.$$

Now we apply Corollary 11 to get:

$$\begin{aligned} f(x_T) - f_* &\leq \frac{1}{2 \sum_{t=1}^T \eta_t} D^2 + \frac{1}{2 \sum_{t=1}^T \eta_t} \sum_{t=1}^T \eta_t^2 \|g_t\|^2 \\ &+ \frac{1}{2} \sum_{k=1}^{T-1} \frac{\eta_k}{\sum_{t=k+1}^T \eta_t} \left(\frac{1}{\sum_{t=k}^T \eta_t} \sum_{t=k}^T \eta_t^2 \|g_t\|^2 \right). \end{aligned}$$

■

By using a worst-case bound of $\|g_t\|^2 \leq G^2$, we obtain:

Corollary 12 If f is G -Lipschitz, then

$$\begin{aligned} f(x_T) - f_* &\leq \frac{1}{2 \sum_{t=1}^T \eta_t} D^2 + \frac{G^2}{2 \sum_{t=1}^T \eta_t} \sum_{t=1}^T \eta_t^2 \\ &+ \frac{G^2}{2} \sum_{k=1}^{T-1} \frac{\eta_k}{\sum_{t=k+1}^T \eta_t} \left(\frac{1}{\sum_{t=k}^T \eta_t} \sum_{t=k}^T \eta_t^2 \right). \end{aligned}$$

F.1 Linear schedule analysis with Theorem 10

In this section, we use Theorem 10 to re-analyze the the linear decay schedule:

$$\eta_t = \frac{D}{G\sqrt{T}} \left(1 - \frac{t}{T+1} \right). \quad (6)$$

The resulting convergence rate is asymptotically correct, but does not achieve the optimal constant obtained by Theorem 3.

Theorem 13 *Schedule 6 gives the following bound on the last iterate:*

$$f(x_T) - f_* \leq \left(2 + \frac{1}{4}\right) \frac{DG}{\sqrt{T}},$$

or more precisely:

$$f(x_T) - f_* \leq \left(2 + \frac{H(T-1) - 2/3}{T+1}\right) \frac{DG}{\sqrt{T}},$$

where $H(T)$ is the T th harmonic sum.

Proof We start with the above bound:

$$\begin{aligned} f(x_T) - f_* &\leq \frac{1}{2 \sum_{t=1}^T \eta_t} D^2 + \frac{G^2}{2 \sum_{t=1}^T \eta_t} \sum_{t=1}^T \eta_t^2 \\ &\quad + \frac{G^2}{2} \sum_{k=1}^{T-1} \frac{\eta_k}{\sum_{t=k+1}^T \eta_t} \left(\frac{1}{\sum_{t=k}^T \eta_t} \sum_{t=k}^T \eta_t^2 \right). \end{aligned}$$

Since the $\frac{D}{G\sqrt{T}}$ part of the step size is constant, it can be pulled outside the summations, so we just need to focus on summations involving $\left(1 - \frac{t}{T+1}\right)$. For the first two terms we have in the bound, they simplify

$$\begin{aligned} \sum_{t=1}^T \eta_t &\propto \sum_{t=1}^T \left(1 - \frac{t}{T+1}\right) \\ &= \left(T - \frac{1}{T+1} \sum_{t=1}^T t\right) \\ &= \left(T - \frac{1}{2} \frac{T(T+1)}{T+1}\right) \\ &= \frac{T}{2}. \end{aligned}$$

Similarly,

$$\begin{aligned} \sum_{t=1}^T \eta_t^2 &\propto \sum_{t=1}^T \left(1 - \frac{t}{T+1}\right)^2 \\ &= \sum_{t=1}^T \left(1 - \frac{2t}{T+1} + \frac{t^2}{T+1^2}\right) \\ &= \left(T - T + \sum_{t=1}^T \frac{t^2}{T^2}\right) \\ &= \left(\frac{T(T+1)(2T+1)}{6(T+1)^2}\right) \\ &= \left(\frac{T(T+1)(T+1/2)}{3(T+1)^2}\right) \\ &\leq \frac{T}{3}. \end{aligned}$$

So we have the following bound on the last iterate:

$$f(x_T) - f_* \leq \frac{DG}{\sqrt{T}} + \frac{DG}{3\sqrt{T}} + \frac{G^2}{2} \sum_{k=1}^{T-1} \frac{\eta_k}{\sum_{t=k+1}^T \eta_t} \left(\frac{1}{\sum_{t=k}^T \eta_t} \sum_{t=k+1}^T \eta_t^2 \right).$$

To simplify the remaining term we rely on computer algebra software. SymPy gives:

$$\sum_{k=1}^{T-1} \frac{\eta_k}{\sum_{t=k+1}^T \eta_t} \left(\frac{1}{\sum_{t=k}^T \eta_t} \sum_{t=k+1}^T \eta_t^2 \right) = \left(\frac{D}{G\sqrt{T}} \right) \frac{4T + 6H(T-1) - 4}{3(T+1)}.$$

Where $H(T) = \sum_{t=1}^T 1/t$ is the harmonic sum. So:

$$\begin{aligned} f(x_T) - f_* &\leq \frac{DG}{\sqrt{T}} + \frac{DG}{3\sqrt{T}} + \frac{2DG\sqrt{T}}{3T} + \frac{DG(3H(T-1) - 2)}{3(T+1)\sqrt{T}} \\ &\leq \frac{2DG}{\sqrt{T}} + \frac{DG}{3\sqrt{T}} + \frac{DG(3H(T-1) - 2)}{3(T+1)\sqrt{T}}. \end{aligned}$$

Note that the term $(3H(T-1) - 2)/3(T+1) \leq 1/4$ for all T , so:

$$\frac{DG(3H(T-1) - 2)}{3(T+1)\sqrt{T}} = \frac{DG}{4\sqrt{T}},$$

So combining with the $\frac{DG}{\sqrt{T}} + \frac{DG}{3\sqrt{T}}$ terms, we have:

$$f(x_T) - f_* \leq \left(2 + \frac{1}{4}\right) \frac{DG}{\sqrt{T}}.$$

bounding the harmonic function with a log gives instead:

$$f(x_T) - f_* \leq \frac{2DG}{\sqrt{T}} + O\left(\frac{DG \log(T)}{T^{3/2}}\right).$$

■

Appendix G. Experimental Setup

Our experiments on CIFAR-10, CIFAR-100, ImageNet and RCNN use SGD, and the remaining problems use Adam. We used decoupled weight decay with Adam in each case following standard practice for each problem.

G.1 Convex Experiments

Each dataset is obtained from the LIBSVM repository with used without modifications.

Hyper-parameter	Value	Hyper-parameter	Value
GPUs	1×V100	Decay	0.0
Batch size	16	Optimizer	Adam
Epochs	100	β_1	0.9
Seeds	10	β_2	0.95

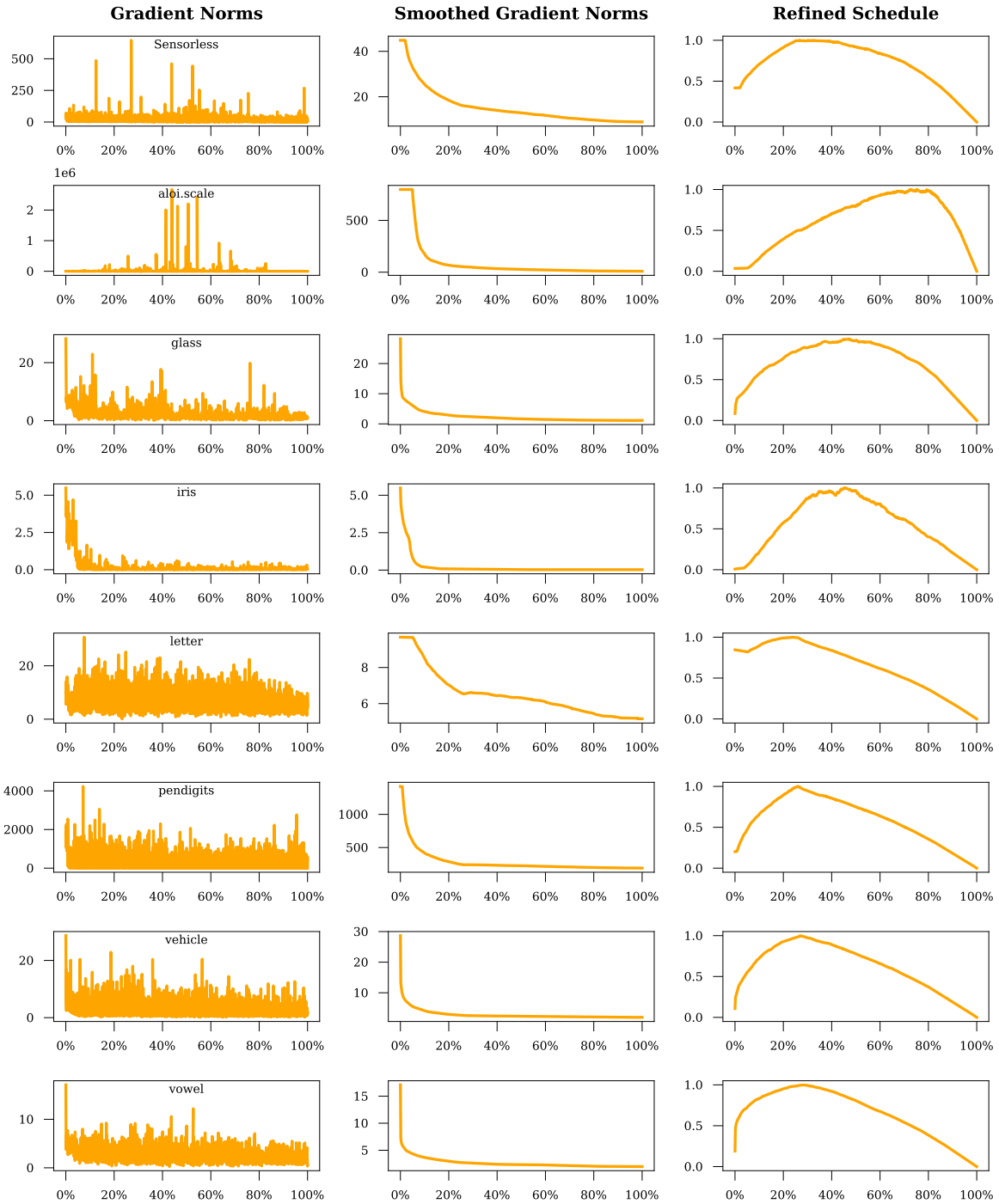


Figure 6: Logistic regression schedules, generated using a linear decay schedule with warmup for the initial run.

G.2 CIFAR-10

We used custom training code based on the PyTorch tutorial code for this problem. Following standard data-augmentation practises, we applied random horizontal flips and random offset cropping down to 32x32, using reflection padding of 4 pixels. Input pixel dataD was normalized by centering around 0.5.

Hyper-parameter	Value
Architecture	Wide ResNet 16-8
Epochs	300
GPUs	1 × V100
Batch size per GPU	128

Hyper-parameter	Value
Seeds	10
decay	0.0001
Momentum	0.9

G.3 CIFAR-100

We used the same codebase as for our CIFAR-10 experiments, with the same data augmentation.

We normalized each input image using fixed mean and standard error values derived from pre-processing the data.

Hyper-parameter	Value
Architecture	DenseNet [6,12,24,16], growth rate 12
Epochs	300
GPUs	1 × V100

Hyper-parameter	Value
Batch size per GPU	64
Seeds	10
Decay	0.0002
Momentum	0.9

G.4 ImageNet

We used the same code-base as for our CIFAR-10 experiments, and applied the same preprocessing procedure. The data-augmentations consisted of PyTorch’s RandomResizedCrop, cropping to 224x224 followed by random horizontal flips. Test images used a fixed resize to 256x256 followed by a center crop to 224x224.

Hyper-parameter	Value
Architecture	ResNet50
Epochs	100
GPUs	8 × V100
Batch size per GPU	32

Hyper-parameter	Value
Seeds	5
Decay	0.0001
Momentum	0.9

G.5 IWSLT14

We used the FairSeq framework¹ for our experiments here, as well as for our GPT and RoBERTa experiments. Rather than a vanilla LSTM we use the variant from (Wiseman and Rush, 2016) provided in the FairSeq codebase.

Hyper-parameter	Value
Architecture	lstm_wiseman_iwslt_de_en
Max Epoch	55
GPUs	1 × V100
Tokens per batch	4096
Warmup steps	4000
Dropout	0.3
Label smoothing	0.1

Hyper-parameter	Value
Share decoder, input, output embed	True
Float16	True
Update Frequency	1
Seeds	10
Decay	0.05
β_1, β_2	0.9, 0.98

1. <https://github.com/facebookresearch/fairseq>

G.6 RoBERTa

The RoBERTa implementation in FairSeq is the canonical one. We differ from the paper’s results by training for a shorter duration, which is necessary to keep our experiments computationally tractable. Our BookWiki dataset matches the original paper.

Hyper-parameter	Value
Architecture	roberta_base
Task	masked_lm
Max updates	23,000
GPUs	$8 \times V100$
Max tokens per sample	512
Dropout	0.1
Attention Dropout	0.1
Max sentences	16

Hyper-parameter	Value
Warmup	10,000
Sample Break Mode	Complete
Float16	True
Update Frequency	16
Seeds	5
Decay	0.0
β_1, β_2	0.9, 0.98

G.7 GPT

Since the training dataset for GPT models are not available, we use the BookWiki dataset as used for RoBERTa training. Our model here is small, using 12 decoding layers and a decoder embedding dim of 768, giving 162 million parameters.

Hyper-parameter	Value
Architecture	transformer_lm_gpt
Task	language_modeling
Max updates	65,000
GPUs	$8 \times V100$
Tokens per sample	512
Dropout	0.1
Attention Dropout	0.1
Max sentences	1
Warmup	10,000

Hyper-parameter	Value
Sample Break Mode	Complete
Share decoder, input, output embed	True
Float16	True
Update Frequency	16
Seeds	5
Decay	0.005
β_1, β_2	0.9, 0.98

G.8 ViT

Our implementation uses the PyTorch Image Models library ², with hyper-parameters following examples given in the repository.

Hyper-parameter	Value
Model	vit_tiny_patch16_224
GPUs	$8 \times V100$
Epochs	300
Batch Size	512
Warmup epochs	5
Hflip	0.5
aa	rand-m6-mstd0.5
mixup	0.1

Hyper-parameter	Value
mixup	0.1
cutmix	1.0
Crop Pct	0.9
BCE Loss	True
Seeds	5
Decay	0.1
β_1, β_2	0.9, 0.999

2. <https://github.com/rwightman/pytorch-image-models>

G.9 DLRM

We used a custom implementation of the DLRM model based on the publicly available code. Our optimizer uses dense gradients for implementation simplicity, although sparse-gradients using AdaGrad is a more common baseline on this problem, we consider AdaGrad variants of our scheduling approach as future work.

Hyper-parameter	Value
Iterations	300 000
Batch Size	128
Emb Dimension	16
GPUs	8×V100

Hyper-parameter	Value
Seeds	5
Decay	0.0
β_1, β_2	0.9, 0.999

G.10 MRI

We used the version of the the fastMRI code base at https://github.com/facebookresearch/fastMRI/tree/main/banding_removal. Note that we found that training failed using PyTorch 2 or newer, and so we ran these experiments using PyTorch 1.9.

Hyper-parameter	Value
Architecture	12 layer VarNet 2.0
Epochs	50
GPUs	8×V100
Batch size per GPU	1
Acceleration factor	4

Hyper-parameter	Value
Low frequency lines	16
Mask type	Offset-1
Seeds	5
Decay	0.0
β_1, β_2	0.9, 0.999

G.11 RCNN

Our RCNN experiments use Detectron2³, and we use a pretrained ResNet backbone⁴.

Hyper-parameter	Value
Backbone	ResNet-50
Max Iter	200000
IMS Per Batch	16

Hyper-parameter	Value
GPUs	8×V100
Momentum	0.9
Decay	1.5e-4

3. <https://github.com/facebookresearch/detectron2>

4. [detectron2://ImageNetPretrained/MSRA/R-50.pkl](https://github.com/facebookresearch/detectron2/blob/master/detectron2/configs/ImageNetPretrained/MSRA/R-50.pkl)